Universiteit Utrecht

CRC FOR GREENHOUSE GAS TECHNOLOGIES

Advanced Reservoir Characterisation for Geological Sequestration of CO_2: Surat Basin Demonstration Project

J.J. Ravestein Bsc.

MSc. Thesis May 2013

Supervisors CSIRO: Dr. C.M. Griffiths

Dr. K. Michael

Supervisor UU: Prof. Dr. C.J. Spiers

Abstract

It is generally accepted that underground geological storage of CO_2 (GSC) in deep aquifers, is the option with the highest potential storage capacity. Detailed subsurface models with a high level of subsurface understanding are required for both estimation of CO_2 storage capacity and GSC site characterisation. To attain this high level of subsurface understanding, models need extensive well data and good 3D seismic coverage, often not available at potential GSC sites. The technology of Stratigraphic Forward Modelling (SFM) has advanced to the stage where numerical simulation of the depositional processes can be used to predict reservoir properties at appropriate scales, away from wells and below seismic resolution. With these predictive qualities, SFM could potentially provide the subsurface understanding required in GSC, even in locations with limited well data and no seismics. This study assesses and demonstrates the potential role of SFM in rapidly generating a well-constrained static reservoir model for generic use in the GSC workflow. The eastern Australian Surat Basin is considered a highly prospective basin for GSC with several potential GSC sites. CSIRO's Sedsim SFM package has been used to create a stratigraphic forward model of the Surat Basin, including a high resolution nested model of the EPQ-7 CO_2 sequestration tenement located in the basin. The model simulates deposition and burial of the Early Jurassic Precipice Sandstone, Early to Middle Jurassic Evergreen Formation and Middle Jurassic Hutton Sandstone. A SFM workflow is devised, in which model results are translated to (pseudo)gamma ray values, to be directly compared to gamma ray well logs. This workflow enables an efficient model-to-well tuning process. The model is based on literature describing the depositional processes in the basin, followed by a process of tuning the model to limited well data. In the basin centre and EPQ-7 tenement, the model results display a good match with well data. The model-generated porosity and permeability values are reasonable, yet could use further refinement. Several potential applications in further GSC workflows are proposed for the model. Finally, it is concluded that this study demonstrates the high potential value of SFM, using Sedsim, in rapidly generating static reservoir models for use in GSC workflows, especially in areas with limited well data.

Contents

1. Introduction

1.1. Aim

Underground geological storage of CO_2 (GSC) is regarded as a potentially important technology to mitigate anthropogenic CO_2 emissions into the atmosphere. The three main underground storage options for CO_2 are: storage in depleted oil and gas reservoirs, storage in deep (saline) aquifers and storage in deep un-minable coal seams (IPCC, 2005). It is generally accepted that CO_2 storage in deep aquifers is the option with the highest potential storage capacity (IPCC, 2005; Bradshaw et al., 2007; Michael et al., 2009).

The estimation of potential CO_2 storages capacities in deep aquifers is very complex due to the various trapping mechanisms involved. Because of the likely dominance of migration assisted storage (MAS, see section 1.2) trapping and its dynamic, time dependent nature, the CO_2 capacity has to be estimated at a certain point in time, and can only be achieved through numerical modelling. This aspect, and the level of detail and resolution required make estimation of CO_2 storage capacity only practical at local and site-specific scales (Bachu et al., 2007). Michael et al. (2009) describe GSC site characterization as the most time consuming and costly part of CO_2 storage site selection process. GSC site characterization requires greater detail than basin assessment investigations with typical steps being: structural and stratigraphic interpretations based on available subsurface data, building of geological models with realistic stratigraphic heterogeneity, and flow simulations to predict CO_2 plume migration (Michael et al., 2009).

The technology of Stratigraphic Forward Modelling (SFM) has advanced to the stage where numerical simulation of the depositional processes can be used to predict reservoir properties at appropriate scales, away from wells and below seismic resolution. Because of the complex nature of deep aquifer GSC in both CO_2 storage capacity estimations and GSC site characterization, greater levels of sub surface understanding are necessary, compared to traditional oil and gas exploration and production. More specifically, realistic subsurface geological models producing realistic property distribution are necessary for numerical flow modelling of CO_2. In this context, stratigraphic forward modelling could be an invaluable tool in the GSC characterisation workflow.

In this study, CSIRO's Sedsim has been used to create an SFM of the Precipice Sandstone, Evergreen and Hutton Sandstone formations of the eastern Australian Surat Basin, in order to assess and demonstrate the potential role of SFM in rapidly generating a well-constrained static reservoir model for generic use as part of the GSC workflow.

1.2. GSC trapping mechanisms and conditions

At short timescales after injection, CO_2 gas or supercritical fluid is trapped by physical mechanisms. At longer timescales, chemical trapping mechanisms such as mineralization and dissolution start playing a role (IPPC, 2005). Bachu et al. (2007) subdivides physical trapping into two types: static trapping, the trapping in stratigraphic or structural traps including (depleted) oil and gas field; and dynamic trapping, residual gas trapping in the pore space at irreducible gas saturation. Residual gas trapping is included in migration assisted storage (MAS) by Bradshaw et al. (2009) and can theoretically store enormous

quantities of CO_2 on the short to medium term in the absence of subsurface closures (Bradshaw et al., 2009; Hodgkinson and Grigorescu, 2012). The primary trapping mechanism of MAS is residual gas trapping in the tail of a migrating plume, trapping in small enclosures at the reservoir/seal interface is considered the secondary mechanism (Bradshaw et al., 2009). The migrating CO_2 plume could potentially reach the surface, although, under favourable conditions, this would take tens of thousands to millions of years. In this timeframe the CO_2 is likely to be trapped by the various physical and chemical trapping mechanisms (Bachu et al., 2007).

In their assessment of GSC suitability of Queensland basins, Bradshaw et al. (2009) stated several conditions necessary for potential GSC:

- Reservoir and seal intervals must be present at depths of at least 800 m.
- The prospective basin did not experience extensive deformation.
- Reservoir properties of greater than 10% porosity and 5 mD permeability.
- Seal intervals must be thicker than 50 meters over 2000 m^2 for conventional seals or 100 m over 2000 m^2 for unconventional seals.

Conventional seals are similar to petroleum geology seals, close to 100% physical barriers to flow, unconventional seals simply slow the CO_2 migration sufficiently to allow physical and chemical trapping mechanisms to ultimately trap the CO_2.

1.3. Stratigraphic Forward Modelling

In stratigraphic forward modelling (SFM) an assumed understanding of sedimentation processes is used to attempt to predict the state of a system at some time in the future (Griffiths, 2008). SFM enables the study of combined influence of a variety of interdependent basin processes at geological time scales, with results reflecting possible changes in sediment distribution over time as a function of the changing depositional environment (Wijns et al., 2004).

A stratigraphic forward model can start at any moment in time, for instance if a simulation starts in the Cretaceous and runs forward for a couple million years, it will predict a portion of the stratigraphic record over the chosen area. If the same model is applied over shorter periods at the present day, the model is predicting the response of a current coastal, fluvial or lacustrine system to environmental forcing. At either scale, the physics are assumed to be the same, and the physical processes that are observed today are assumed to have also operated in the geological past (Griffiths, 2008).

The results of SFM simulations can be compared with actual subsurface data to provide a better understanding of regional and local sedimentary basin development, to test new play concepts, complement and constrain tectonic, sequence and seismic stratigraphic interpretations and to gain a better appreciation of reservoir geometries and facies architecture. During this process, the need to carefully quantify geological processes as input parameters can greatly enhance process and palaeo-environmental understanding (Griffiths, 2001).

1.4. Sedsim

CSIRO's Sedsim is a 3D numerical hydraulic process-response stratigraphic forward modelling package that simulates sediment transport, deposition and erosion by solving a numerical approximation to the Navier-Stokes fluid flow equations. Sedsim was originally developed at Stanford University with the conceptual background described by Tetzlaff and Harbaugh (1989). Since then, it has undergone several generations of modification, first at the University of Adelaide and later at CSIRO. The core Sedsim flow and sedimentation programs are linked to modules including: subsidence, sea level change, wave transport, aeolian deposition, compaction, slope failure, organics and carbonates (Wijns et al., 2004).

Sedsim has seen use in a wide range of research (Wijns et al., 2004; Salles et al., 2010; Huang et al., 2012), from hydrocarbon exploration (Griffiths and Paraschivoiu, 1998; Griffiths and Dyt, 2001; Griffiths et al., 2001) to predicting effects of future climate change (Li et al., 2007; Li et al., 2009). Recently, where Miranda et al. (2012) used Sedsim in a GSC workflow, Sedsim simulated data was used to complement a geocellular model in areas with no data.

The following section on fluid-flow equations and sediment transport in Sedsim, is based on studies by Griffiths and Paraschivoiu (1998), Paraschivoiu et al. (2000), Wijns et al. (2004) and Miranda et al. (2012).

The complete Navier-Stokes equations describing fluid flow in three dimensions are impossible to solve due to limited computer speeds. In order to overcome this problem, Sedsim simulates continues flow using the concept of isolated fluid elements (Tetzlaff & Harbaugh 1989). This Lagrangian approach to the hydrodynamics allows for a massive increase in speed of computation and simplification of the fluid flow equations. The fluid elements are treated as discrete points with a fixed volume that travel over an orthogonal grid describing the topographical surface. In this marker in cell approach, fluid elements can carry a sediment load, as the fluid elements interact with the topography, sediment deposition, erosion and transport is simulated.

Sediment is transported across the surface of the model, in which it bypasses the surface, or is deposited on the surface, according to the principles of conservation of mass. So for each time interval:

sediment in + sediment eroded = sediment in the fluid + sediment deposited + sediment out

The boundary between erosion and transportation is determined by the critical shear stress, calculated as a function of particle diameter and density. The rate of sediment deposition or erosion is proportional to the excess effective sediment concentration. The effective sediment concentration is the difference between the actual sediment load within a fluid element and its sediment-carrying capacity. The sediment-carrying capacity of a fluid element is an empirical function of the parameters involved in the flow, such as water density, velocity, fall rate of the contained sediment and buoyancy of the flow. The fluid element movement is determined by its interaction with the topographic surface, its density, whether it is undergoing hypo- or hyperpycnal flow and which grain-sizes are moving as bed load or as suspended load.

Fluid elements are released into the model from sediment sources at a chosen time and location with an initially specified sediment load and velocity. At each time step the position and velocity of each fluid element are recalculated, and the sediment transfer between the surface and the fluid element is calculated at the grid nodes. After deposition, sediment can still be transferred due to local unstable slope angles and will be diffused through multiple neighbouring grid cells until a stable slope angle is reached. This process, repeated over time steps from seconds to millions of years, results in a 3D sediment package built forward in time from an initial depositional surface at lateral scales from centimetres to hundreds of kilometres.

Sedsim is controlled by a parameter input file allowing for easy editing and viewing of the various input parameters used and it specifies which modules will be turned on or off in the simulation. The input file contains links to additional files necessary for Sedsim core and module operation, files such as basement topography-, tectonics-, sea level curve files. Sedsim can simulate four user defined siliclastic grain-sizes and the in-situ accumulation of two types of organics and carbonates. After the simulation, visualization files can be generated allowing model visualization in the Sedview 3D viewer. In Sedview the user can scroll through time and display information such as grain size, porosity, sediment age and facies. The sediment can be displayed solid, or with single or multiple X or Y-direction cross-sections (fences).

2. Geological setting

The Surat Basin is a large eastern Australian basin (figure 2.1), located largely in Queensland and to a lesser extend in New South Wales. Unconformably overlying the Permian-Triassic Bowen Basin, it contains up to 2500 m of continental Jurassic and marine Cretaceous sediment and has an approximate area of 300 000 km^2 (Exon, 1976). The Surat Basin sediments are generally flat lying and undeformed, with only mild folding at places (Reza et al., 2009). The Basin has an erosive boundary to the north, where most of the Surat and Bowen sediment succession is exposed at the surface.

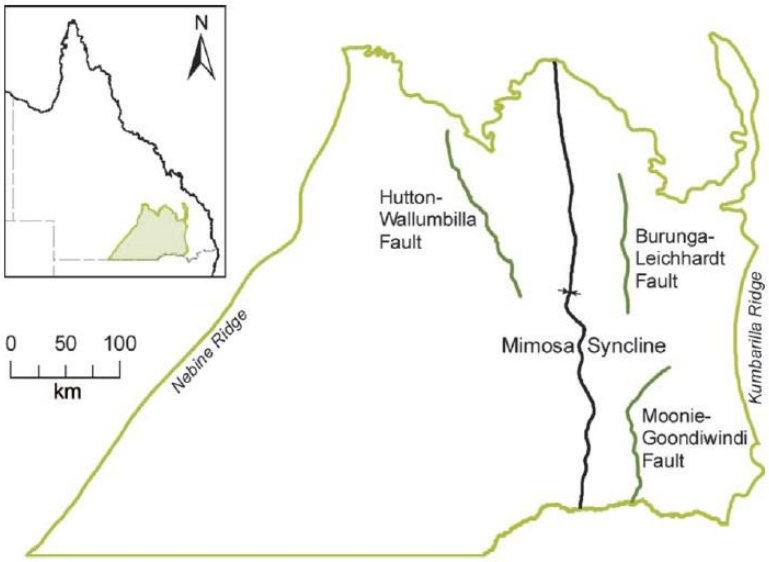

Figure 2.1: Location of the Surat Basin and its main structural features (from Hodgkinson and Grigorescu, 2012).

The Surat Basin is part of a large intracratonic sag, which eventually formed the Great Artesian Basin. A number of shallow platform basins were formed as a result, including the Surat, Clarence-Moreton and Eromanga basins (Green, 1997). Because of this, Surat sediments generally extend well beyond the Surat Basin and are often present in, or interfinger with, formations in surrounding basins (Wiltshire, 1989; Elliot, 1989).

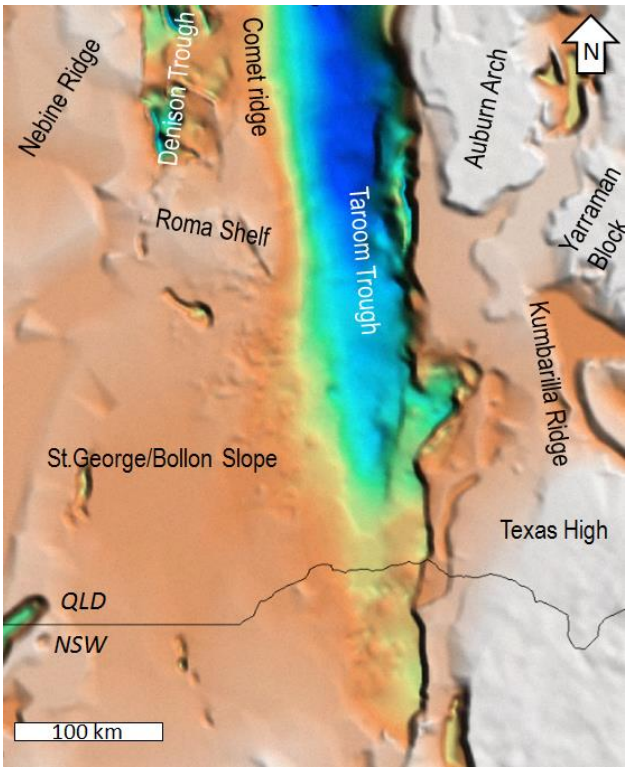

Figure 2.2: Surat Basin basement features are clearly visible on a depth to basement map, color indicates basement depth: blue (deep) to white (shallow) (FrogTech, 2005).

The Early Jurassic Surat Basin is dominated by terrestrial sedimentation in fluvial to lacustrine depositional systems in which three upwards-fining cycles are identified (Exon, 1976; Green, 1997; Hoffman et al., 2009; Totterdell et al., 2009). These cycles consist of high energy environment sandstones grading gradually into low energy environment deposits, often silts and coals. The formations associated with the cycles are (figure 2.3): Precipice Sandstone – Evergreen Formation in the Early to Middle Jurassic, Hutton Sandstone – Walloon Coal Measures in the Middle to Late Jurassic and Springbok Sandstone – Westbourne Formation in the late Jurassic.

The Bowen Basin and the Palaeozoic blocks that surround the Bowen Basin, act as basement to the Surat Basin (Exon, 1976). The Surat Basin is contiguous with the Clarence-Moreton Basin in the east and Eromanga Basin in the west, with basin margins defined by the Kumbarilla Ridge in the east and Nebine Ridge in the west (figure 2.2) (Green, 1997). Positive features in the Early Jurassic consisted of elevated basement blocks in the southwest (St. George Slope), northeast (Auburn Arch, Yarraman block) and southeast (Texas High) (Exon, 1976).

The Surat Basin is largely underlain by the Taroom Trough (figure 2.2). This Bowen Basin structure is filled with Permian and Triassic sediment. The boundaries of the Taroom Trough largely define the Bowen Basin margins. The trough is bound to the east by the Goondiwindi-Moonie and Burunga-Leichart thrust faults and to the west by the Hutton Wallumbilla Fault, St George Slope, Roma Shelf and Comet Platform. Directly above the Taroom trough, the Surat Basin sediments form a large syncline

named the Mimosa Syncline. The Surat succession is thickest along the axis of the syncline, which is parallel to the Taroom Trough axis.

2.1. Tectonics

In the Middle to Late Triassic, compressive deformation resulted in regional uplift and erosion of the Bowen Basin, with up to 3000m of succession missing (Fielding et al., 1990). This period of extensive erosion produced a marked peneplain, on which the Surat Basin sediments were deposited (Green, 1997; Korsch and Totterdell, 2009). The resulting unconformity, the basal Jurassic unconformity, separates the Surat Basin from the Bowen Basin sediment and Palaeozoic basement. The duration of the hiatus associated with this unconformity increases to the west (Tabassi, 1986; Golyn and Smyth, 1986) and represents an approximate 20 Ma (Battersby, 1981) to 30 Ma of missing strata (Reza et al., 2009).

Korsch and Totterdell (2009) describe the Jurassic subsidence of the Surat Basin as extremely slow compared to the underlying Bowen Basin, resulting in a relative thin sediment package that accumulated over a relative long time period. Tectonic subsidence curves for the Surat Basin indicate that the rate of subsidence during the Jurassic did not vary significantly (Korsch and Totterell, 2009).

Dynamically induced platform tilting (Mitrovica, 1989) due to viscous mantle corner flow above a west dipping subduction zone is thought to be the mechanism behind the Surat Basin's slow and widespread subsidence (Gallagher, 1990; de Caritat, 1992; Gallagher, 1994). The broad intracratonic downwarp, following from the platform tilting, resulted in the Surat Basin only experiencing minor deformation and mainly passive subsidence. Waschbusch et al. (2009) demonstrated that subsidence due to dynamic platform tilting included both a near-field effect in the eastern Surat Basin and a far-field effect in the western Surat Basin.

Sedimentation continued into the Cretaceous. Initial increased subsidence rate during the Early Cretaceous was followed by a Middle Cretaceous compressional event (Gallagher et al., 1994). This compression induced regional uplift and reactivated the Permian-Triassic Moonie-Goondiwindi, Burunga-Leichhardt and Hutton-Wallumbilla fault systems (figure 2.1). The movement along these fault systems produced several small anticlinal structures to the east of the basin (Hodgkinson and Grigorescu, 2012) but no brittle displacement along the faults (Korsch et al., 2009). Korsch et al (2009) consider the compressional event to have occurred between 95 Ma and 90 Ma, in the Early Late Cretaceous.

Several studies use apatite fission track methods to estimate the thickness of sediment removed by the extensive erosion caused by the Cretaceous compressional event: Raza and others (2009) estimated 1.5 km of section lost in the southern Taroom Trough, Marshallsea (1985) estimated 3 km north of the Taroom Trough. Furthermore, Gallagher et al (1994) found 2.5 km and 1 km respectively on the eastern and western flanks of the Surat Basin. This uplift and erosion very likely resulted in most of the present day erosional boundaries of the Surat Basin and the outcropping of Bowen Basin sediment to the north as Power and Devine (1970) estimated the original northern depositional boundary of the Surat Basin to be at least 120 kilometres further north.

2.2. Stratigraphy

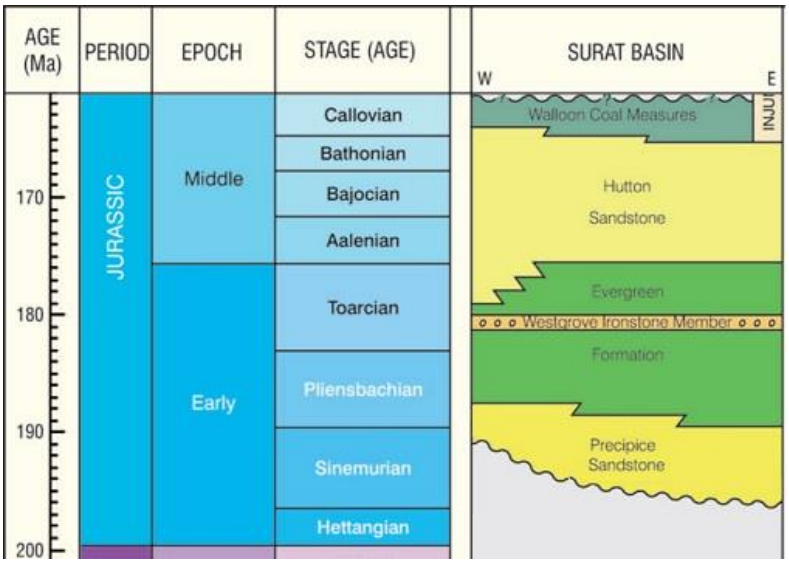

Figure 2.3: Early to Middle Jurassic stratigraphic column of the Surat Basin (modified from Hodgkinson and Grigorescu, 2012).

2.2.1. Precipice Sandstone

Exon (1976) divided the Precipice Sandstone into two subunits: a coarse grained lower unit and a finer grained upper unit. The Precipice Sandstone as described by Green et al. (1997) is mostly equivalent to the lower (coarser) unit of Exon (1976). This is a source of some confusion as it is not always clear what division is used in publications and reports. To complicate things further, in the basal part of the Evergreen Formation a coarse grained sandy interval can be present. According to Green et al. (1997) the top of the Precipice Sandstone should be taken where the highest massive porous quartzose sandstone underlies the less porous sublabile sandstones and mudstones of the Evergreen Formation. The Precipice Sandstone is of Early Jurassic age, approximately 202-194.5 Ma (Korsch and Totterell, 2009). Based on palynological data (Reiser and Williams, 1967), Martin (1981) concluded that the formation base is diachronous and decreases in age to the west, onto the St. George slope and Roma shelf. In the Mimosa Syncline, the Precipice Sandstone has a maximum porosity of 36.9% and median porosity of 17.9% (Bradshaw, 2009).

Lithology

The lower subunit of the Precipice Sandstone is a medium to coarse grained, porous and permeable quartz sandstone (Martin, 1981). It is thickly bedded, cross stratified, in places pebbly and conglomeritic interbeds may be present. The sandstone is mostly quartzose with minor lithic grains, feldspar, muscovite, mica, coaly fragments, abundant red garnet in some horizons and the matrix consists of authigenic clay and silica (Exon, 1976).

The upper unit consists of fine to medium grained, thinly bedded, sublabile, semi porous sandstone and siltstones (Green, 1997). The siltstone is generally laminated, with thin seams of coal and carbonaceous shale (Exon, 1976). Martin (1981) described the upper unit sandstones in the Roma area as:

mineralogically less mature, containing more mica, feldspar and rock fragments than elsewhere and sometimes cemented by calcite. Power and Devine (1970) found the formation to become sandier towards the western and southern basin edges.

Boundaries

The Precipice Sandstone unconformably overlies Permo-Triassic sediment of the Bowen Basin as well as Devonian to Carboniferous basement rocks. The present day north and northeastern limits of the Precipice Sandstone are erosional and largely at the surface. The formation boundaries to the south, southwest and southeast are due to limit of deposition or zero-edges (Veevers et al., 1982; Elliot, 1993; Martin, 1981; Power and Devine, 1970). The formation terminates against the Auburn Arch and Yarraman Block in the northeast, the New England block and Texas High in the southeast and the St. George Slope in the southwest (Martin, 1980; Exon, 1976). The formation grades laterally into the Helidon Sandstone of the Clarence-Moreton Basin across the Kumbarilla Ridge (Exon, 1976; Green, 1997). The formation is generally absent at the Nebine Ridge, except for the northwest where an outcrop crosses into the Eromanga Basin and is equivalent to the lower basal Jurassic unit of the Eromanga Basin (Exon, 1976; Green 1997). The formation grades gradually into the overlying Evergreen Formation with possible localised truncation of the Precipice Sandstone at the basin margins (Hoffman, 2009).

Thickness and distribution

The Precipice Sandstone reaches thicknesses of over 150 m along the Mimosa Syncline and averages 60-80 m over the entire basin (Hoffman et al., 2009). From the isopach map in figure 2.4 three distinct depocenters can be seen in the Mimosa Syncline and one largely eroded depocenter in the northwest. Sediment thicknesses generally increase to the north, up to the present day erosional boundary. Significant thinning occurs across the Goondiwindi-Moonie and Burunga-Leichart thrust faults onto the eastern upthrown side.

Highest Precipice Sandstone thicknesses are located directly over places where the Bowen Basin succession is thickest, this distribution suggests Early Jurassic deposition was being influenced by compaction of the underlying Bowen Basin sediments (Hoffman et al., 2009). Even though the lithology directly underlying the Precipice Sandstone is largely fine-grained, apatite fission track studies of the area have shown that they would have been buried up to 3000 m before being eroded and peneplained prior to Precipice deposition (Fielding et al., 1990). This makes the assumption that compaction alone forced the correspondence in depocenters unlikely.

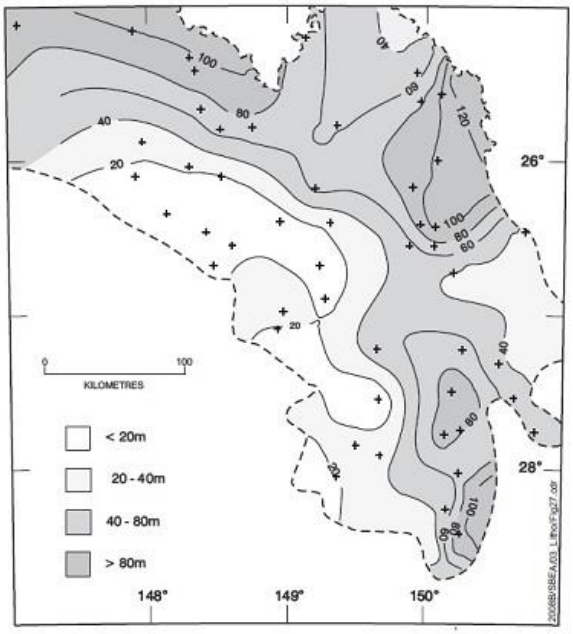

Figure 2.4: Isopach map of the Precipice Sandstone (Green, 1997)

Depositional environment and provenance

The Precipice Sandstone is thought to have been deposited in transverse bars in a braided stream system that, with time, gradually reduced in energy and changed into a meandering river system (Martin 1981, Exon 1976) resulting in the deposition of the coarse lower unit and finer grained upper unit. Palynoflora from the Precipice Sandstone are indicative of a continental environment. In continental sequence stratigraphic terms, Hoffman et al. (2009) concluded that the Precipice Sandstone represents a low stand systems tract.

Martin (1981) proposed that likely gradients of streams depositing the sandstones were respectively 0.001 (1 m/km) and 0.0005 (0.5 m/km) for the braided river streams of the lower Precipice Sandstone, and meandering streams for the last phase of deposition in the upper Precipice Sandstone. Palaeocurrent data have only been measured along the northern outcrop (Exon, 1976; Martin, 1981) and on the Roma Shelf (Sell, 1972), suggesting streams flowing in an easterly direction in the north and north-easterly direction on the Roma shelf. No study has been done into palaeocurrent directions for the rest of the basin and has resulted in speculation over the provenance of the Precipice Sandstone. Proposed sources of the Precipice Sandstone are:

A) Local basement highs that surrounded the basin, namely: Auburn Arch, Yarraman Block, Texas high (New England block) and St. George slope (Exon. 1976)(figure 2.5).
B) Western source supplied by sediment from Precambrian rocks to the west, south of the Eromanga Basin, with a minor source in the southeast supplied by the New England Fold Belt (Martin, 1981).
C) A north and/or western garnet rich source, supplying the quartzose sandstone formations in the Surat and Bowen basin (Wiltshire, 1989).

D) South-Eastern Precipice composition points at a granitic source rock, its distribution pattern suggesting east or southeast sediment transport, probably sourced by the Auburn, Yarraman and New England blocks (Tabassi, 1986).

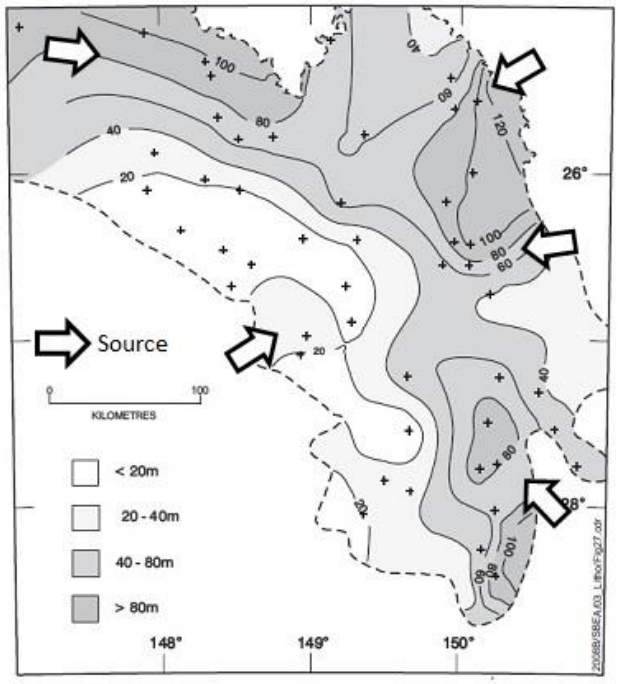

Figure 2.5: Sources of the Precipice Sandstone based on the proposed provenances, modified from Green (1997

2.2.2. Evergreen Formation

The Evergreen Formation overlies the Precipice Sandstone and can be divided into three intervals: Lower Evergreen Formation, Boxvale Sandstone Member, Upper Evergreen Formation with the Westgrove Ironstone Member. This division is based on differences of depositional environment and rock type. The Evergreen Formation is dated to be of Early to Middle Jurassic age, roughly 194.5 to 178 Ma (Korsch and Totterell, 2009). The formation is known to seal hydrocarbon accumulations, although the Boxvale Sandstone Member has a maximum porosity of 33.4% and median porosity of 15.9% at the Roma Shelf (Bradshaw, 2009).

Lithology

From Green et al. (1997): The Lower Evergreen Formation comprises fine to medium grained sandstone, carbonaceous mudstone and minor carbonaceous siltstone, shale and coal. The Boxvale Sandstone Member commonly comprises thinly to thickly bedded, fine to coarse-grained, cross-bedded, quartzose sandstone, with some argillaceous clay matrix. Intervals of thinly bedded, very fine-grained, porous quartzose sandstone with carbonaceous siltstone, shale and coal interbeds also occur. The upper Evergreen Formation between the Boxvale Sandstone Member and the base of the Hutton Sandstone mainly comprises dark grey to black mudstone, laminated with sandstone, siltstone and shale and fine-grained, sublabile to labile sandstone. The Westgrove Ironstone Member forms the lower part of this

interval and comprises interbedded mudstone and chamositic mudstone with a pelletal or oolitic structure, sideritic cement, and minor sandstone.

Most of the sandstones in the Evergreen Formation are impermeable due to the presence of an argillaceous matrix and calcareous and ferruginous cements (Exon, 1976). The argillaceous matrix reduces permeability and porosity and can be the result of autogenic kaolinite generated from lithic clasts in the Evergreen Formation sands, although the dissolution of micas and feldspars results in good secondary porosity in places (Butcher, 1992).

Boundaries

The Evergreen Formation is generally thought to conformably overlie the Precipice Sandstone (Exon, 1976; Golyn and Smyth, 1986; Green, 1997). Although at the basin margins the transition is less gradual and even unconformable (Hoffman 2009). At locations beyond the depositional limits of the Precipice Sandstone, the formation unconformably overlies Bowen Basin strata or pre-Permian basement.

To the east, the Evergreen Formation is laterally continuous with the Marburg Sandstone of the Moreton Basin near the Kumbarilla Ridge (Gray, 1972) and Yarraman Complex (Exon, 1976). Compared to the Precipice Sandstone, the depositional boundaries of the Evergreen Formation extend further onto surrounding highs, such as the St. George slope, Texas High and Kumbarilla Ridge (Exon, 1976). The northern boundary of the formation is erosive and it outcrops south of the Precipice Sandstone exposure.

Thickness and distribution

The Evergreen Formation is more uniform in thickness than the Precipice Sandstone and extends beyond the boundaries of the Precipice Sandstone. Maximum thicknesses are just over 300 metres with the Mimosa Syncline forming the main axis of deposition (figure 2.6) (Green, 1997).

Generally, the silt and mudstone percentages increase towards the basin centre, roughly towards the Mimosa Syncline. In the western and eastern margins of the basin the percentage of sandstone is higher than in other areas, probably due to closer proximity to the sediment sources (Green, 1997; Butcher, 1992). Sandstone content is particularly high in the Basal Evergreen Sands in the lower Evergreen Formation on the Roma Shelf on the western margin (Bradshaw et al., 2009, Butcher, 1992).

The Boxvale Sandstone Member is deposited somewhat towards the basin margins on the western and eastern flanks of the Mimosa Syncline (Cadman et al., 1998; Green, 1997) and can have a thickness of 25 m (Bradshaw, 2009) to 40 m (Exon, 1976). The overlying Upper Evergreen Formation contains the Westgrove Ironstone Member followed by a succession of mud- and siltstone (Exon, 1976) and is spatially more extensive than the Boxvale Sandstone (Hoffman, 2009).

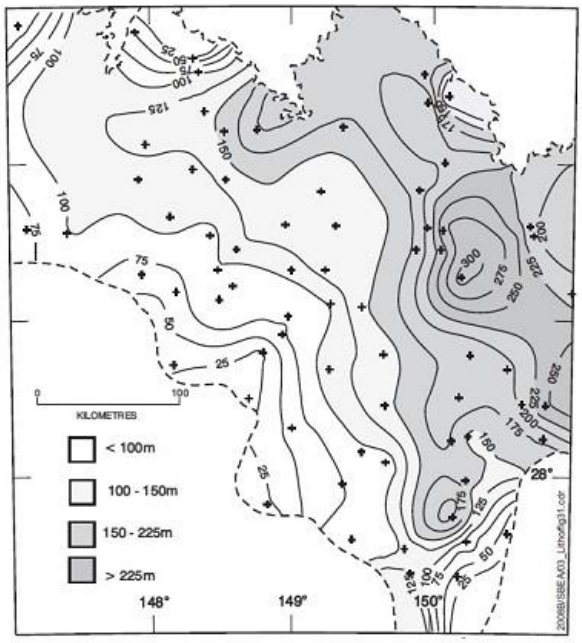

Figure 2.6: Isopach map of the Evergreen Formation (Green, 1997)

Depositional environment and provenance

The Lower Evergreen Formation was probably deposited by meandering streams, although interpretations differ on whether the streams interacted with freshwater lakes (Mollan et al., 1972; Butcher, 1992) or formed part of a coastal plain with deltas (Exon, 1976). The Basal Evergreen Sands present in the western part of the basin were probably deposited by higher energy streams (Butcher, 1992). Because of the lateral relationship with the Evergreen Formation, it is very likely that the Helidon Sandstone of the Moreton Basin, would have been deposited by the same sort of higher energy streams at roughly the same time (Butcher, 1992).

The coarse, thick bedded, cross stratified sandstones of the lower part of the Boxvale Sandstone Member are stream deposits (Exon, 1976; Butcher, 1992). The upper part of the Boxvale Sandstone Member is interpreted as lacustrine shoreline deposits (Mollan et al., 1972), which were possibly part of a prograding lacustrine delta (Fielding, 1989; Browne and Hart, 1990). Thickest sand build-ups are adjacent to the shorelines of the water body, which had migrating shorelines, although it is not known whether the water body was a large discrete lake or a series of small lacustrine sub basins, or what the relation was with the ocean to the east (Butcher, 1992; Fielding, 1989).

The chamositic, oolitic and mudstone beds of the overlying Westgrove Ironstone Member, part of the Upper Evergreen Formation, may have been the result of gentle wave action coupled with sediment starvation in a reducing environment (Mollan et al., 1972). Brakel (1992) suggested that this, coupled with the widespread deposition of the member, indicated deposition at a time of maximum flooding. The very fine-grained nature of the sediment on top of the Westgrove Ironstone Member seems to support such a low energy depositional environment.

Paleocurrent data indicate flow west to east for most of the basin (Exon, 1976; Butcher, 1992; Green, 1997) although some input from the east is to be expected due to the interfingering with Moreton Basin sandstones and the presence of Boxvale Sandstone near the eastern margins. Most of the Evergreen Formation is thought to be sourced from metamorphic rocks, while the Boxvale Sandstone would be sourced from earlier quartz rich formations or granites (Butcher, 1992).

2.2.3. Hutton Sandstone

The Hutton Sandstone is of largely Middle Jurassic age, 176 Ma–166 Ma (Korsch and Totterell, 2009), has no members, and is generally not subdivided. The formation has a basin-wide maximum porosity of 34.3% and a median porosity of 17.8% (Bradshaw, 2009).

Lithology

The Hutton Sandstone consists mainly of sandstone with interbedded siltstone and shale and minor mudstone and coal. The sandstone is white to light grey, fine to medium-grained, well sorted, sublabile to quartzose, partly porous with some pebble bands and shale and siltstone clasts in the lower part. Siltstone and shale are light to dark grey, micaceous, carbonaceous and commonly interlaminated with very fine-grained sandstone (Green, 1997).

Boundaries and thickness

According to Exon (1976) the contact between the Hutton Sandstone and underlying Evergreen Formation is conformable. Yet, Hoffman et al. (2009) conclude from well correlations and outcrop data there is evidence that the contact is erosional. Based on the unconformable contact and the abrupt change in grain size and composition, Hoffman et al. (2009) further suggest the contact to be a major sequence boundary formed by a sudden base level fall.

The Hutton Sandstone has a maximum thickness of roughly 265 m close to the Mimosa Syncline axis (figure 2.7)(Green, 1997), and is between 120 and 180 m thick in most of the basin (Exon, 1976). The axis of the depocentre trends northwest compared with the more northerly trend for the older Surat Basin units (Hoffman., 2009). The Hutton Sandstone is regionally a lot more prevalent than the underlying Precipice and Evergreen, and it is present in the Eromanga Basin to the west and is similar to, and grades into, the Marburg Sandstone of the Moreton Basin to the east (Exon, 1976; Green, 1997). As a result the Hutten Sandstone zero-edges extend much further onto highs like the St. George Slope and Texas High. The north and north-eastern boundaries are erosional (Green, 1997; Hoffman, 2009), like the Evergreen and Precipice formations, yet lie further south towards the basin centre.

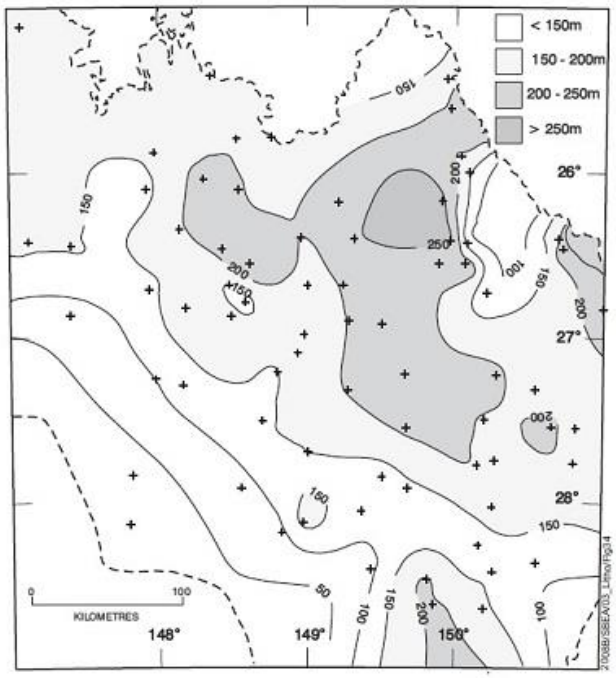

Figure 2.7: Isopach map of the Hutton Sandstone (Green, 1997)

Depositional environment and provenance

The Hutton Sandstone was deposited by meandering rivers on a broad floodplain with generally quartz rich sediments sourced from the northeast, southeast and southwest (Allen, 1976). Due to similarities in sediment composition, it is very likely that the Hutton Sandstone has a similar provenance to the Precipice Sandstone (Wiltshire, 1989). With time, the fluvial energy of the Hutton Sandstone reduced and coal swamps formed, depositing the silt-, mudstone and coal dominated Walloon Coal Measures (Hoffman, 2009; Green, 1997).

2 3. Surat Basin geostorage play

In their assessment of GSC suitability of Queensland basins, Bradshaw et al. (2009) indicated the Surat Basin as a highly prospective basin. Bradshaw et al. (2009) considered the Evergreen Formation a regional seal and the Walloon Coal Measures a potential regional seal. Furthermore, the Precipice Sandstone and Hutton Sandstone were considered regional reservoirs. Other, more spatially restricted, potential reservoirs are the Boxvale Sandstone Member and the Basal Evergreen Sand. The Precipice Sandstone, Evergreen Formation and Hutton Sandstone are all at super-critical storage depths (>800 m) in the south and central Surat Basin (QCGI, 2009).

Bradshaw et al. (2009) estimated the Precipice Sandstone, coupled with the Evergreen Formation acting as seal, to have the highest estimated theoretical storage capacity with 1289 Mt of CO_2, closely followed by the Hutton Sandstone and Walloon Coal Measures (Walloon subgroup) with 1198 Mt.

The best potential storage location in the Surat Basin is considered to be the broad structural depression of the Mimosa Syncline. Here, the strata dip gently upwards, providing a structural architecture that

favors slow, long range migration of CO_2 ideal for migration assisted storage. Other storage options are limited to storage in depleted oil and gas fields in the basin, which provide several orders of magnitude less storage capacity (Bradshaw et al., 2009).

3. Workflow

The main focus of the workflow applied in the project is to achieve the aim of the project as efficiently as possible. This is achieved by gradually increasing the model complexity and detail in conjunction with the increasing knowledge and skill of the modeller. Model complexity is increased by increasing model temporal and spatial resolutions as well as detail in input data such as: sea level, compaction, tectonics and sediment sources. As this process continues, the data against which the model is tested and tuned are increased in detail commensurately. With tuning is meant: the process of comparing the model to subsurface observations and the subsequent adjustment of the model input parameters to improve the match between the model and subsurface observations in the next model iteration.

Figure 3.1 shows a graphic representation of the workflow used. The first step in Stratigraphic Forward Modelling (SFM) is the creation of a conceptual model of the area of interest. The conceptual model exists mainly in the mind of the SFM modeller and incorporates the existing knowledge and data with assumptions and simplifications in order to build the SFM input data. The conceptual model is based on existing literature describing the geology and depositional environments of the Surat Basin as summarised in the preceding chapters. Literature provides information and data necessary to model the depositional processes, such as: depositional environments and palaeogeographic maps, facies distributions, sediment provenance and palaeo-flow directions. Furthermore, information was gathered concerning formation thickness, formation boundaries and sediment burial and erosion.

The information and data from the conceptual model were used to create input data for the Sedsim model. The first model was a coarse resolution model with a 24x17 grid, 25 km grid spacing and time steps of 100k years, and will be referred to as the 'Initial Model'. The modelled interval started with the Precipice Sandstone and was followed, one formation at a time, by the Evergreen and Hutton formations. Results from the model were compared to well-based cross-sections included with the QCGI (2009) report. Following the comparison, model input files such as: sediment source locations, sediment volumes, tectonics and sea levels were tuned to return improved matches to observed formation thickness, sediment type and sediment heterogeneity with the cross-section from QCGI (2009). The relative low spatial and temporal resolution of the model resulted in simulation runtimes of approximately 30 minutes, allowing a rapid series of model iterations.

After returning a satisfactory match to the cross-sections from the QCGI (2009) report, the resolution of the model was increased from 25 km grid spacing in a 24x17 grid to 10 km grid spacing in a 61x44 grid. The temporal resolution was changed from 100k-year time steps to 10k-year time steps. This model with increased spatial and temporal resolution will be referred to as the 'Basin-wide Model' and had simulation runtimes of roughly 10 hours. The increased grid node density allowed for direct model-to-well comparisons, as the grid nodes approximated the well locations much closer than the previous 25 km grid spacing Initial Model. In the model-to-well comparisons, the gamma ray and porosity logs of several wells are compared to Sedsim pseudo-gamma ray and porosity output at the grid node closest to the well location. Using these comparisons the Sedsim model input data was tuned to best fit the well data. The increased temporal resolution simulates more and finer sediment layers, resulting in a better representation of sediment distribution compared to the Initial Model.

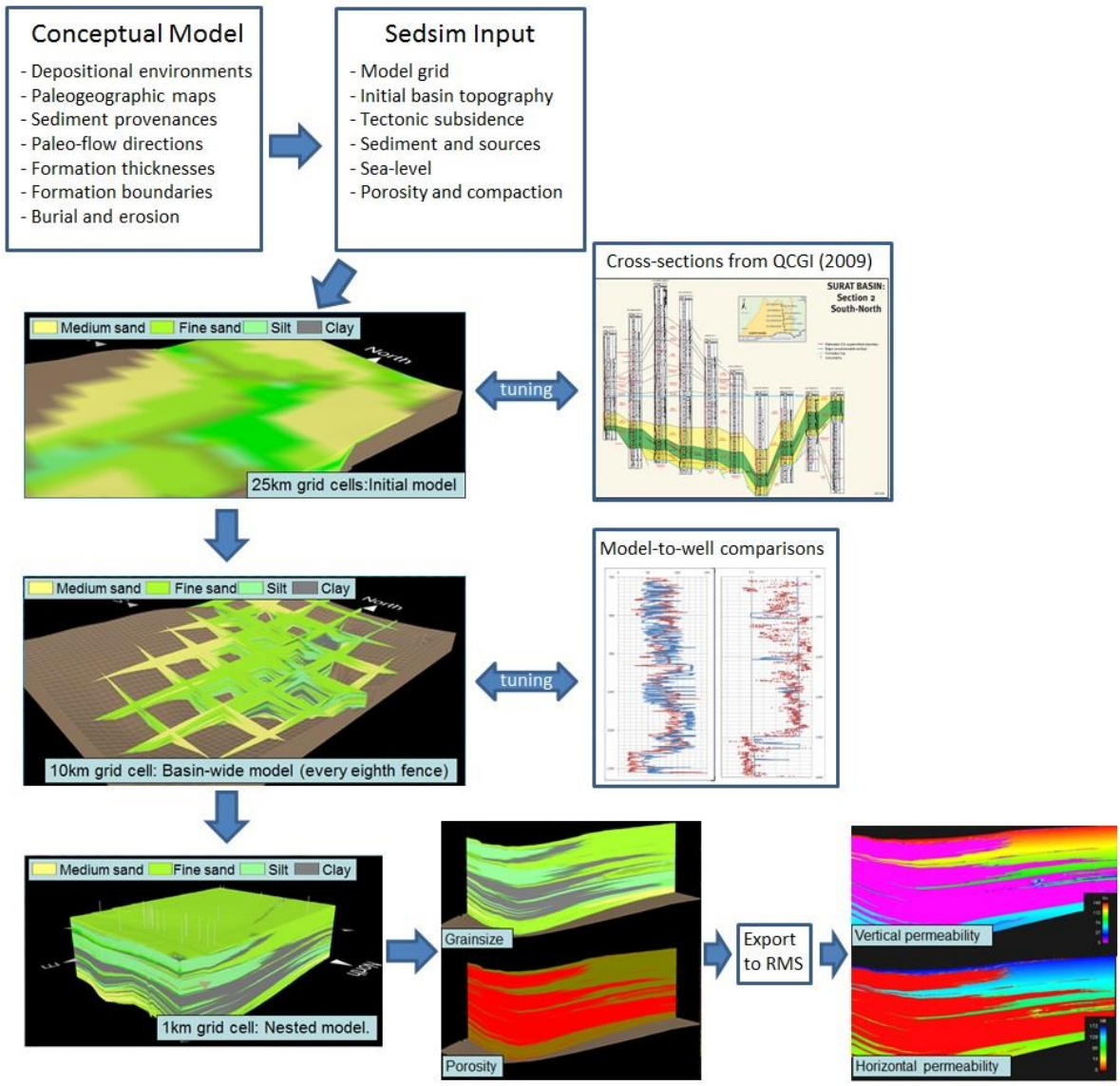

Figure 3.1: Schematic representation of the workflow applied in the project.

Within the Basin-wide Model, a nested simulation was run for the EPQ-7 site, a potential geologic carbon sequestration tenement. At the location of the EPQ-7 site a 61x81 grid with 1 km grid spacing was placed in the Basin-wide Model. Compared to the larger Basin-wide model, the Nested Model uses higher resolution basement topography and tectonics input files. This, combined with the higher spatial model resolution, results in a high data density in the most relevant area of the Surat Basin stratigraphic forward model. The nested model uses the same temporal resolution (10k years) as the larger Basin-wide Model, the addition of the nested model resulted in simulation runtimes of 40 hours.

The final model iterations with the best match with well data were exported in Eclipse format (.GRDECL) and imported into the Roxar RMS reservoir modelling software. In RMS, the Sedsim 3D porosity output was used in combination with a porosity-permeability transform to calculate the horizontal and vertical permeability, for both the Nested, and the Basin-wide Model.

4. Methods

The methods section is subdivided in sections describing the methodology behind:

- Model input data
- Model-to-well comparisons
- Tuning process
- Permeability Model

4.1. Model input data

4.1.1. Model grid and location

Three model grids were used in the project, each with different grid size and grid spacing:

- Initial Model of the Surat Basin, with a grid of 24 rows and 17 columns and a grid spacing of 25 kilometres (575x400 kilometre)
- Basin-wide Model of the Surat Basin, with 61 rows and 44 columns and a grid spacing of 10 kilometres (600x430 kilometres) (figure 4.1,4.2)
- Nested Model of the EPQ-7 potential CO_2 sequestration tenement, with 61 rows and 81 columns and a grid spacing of 1 kilometre (80x60 kilometres) (figure 4.1,4.2)

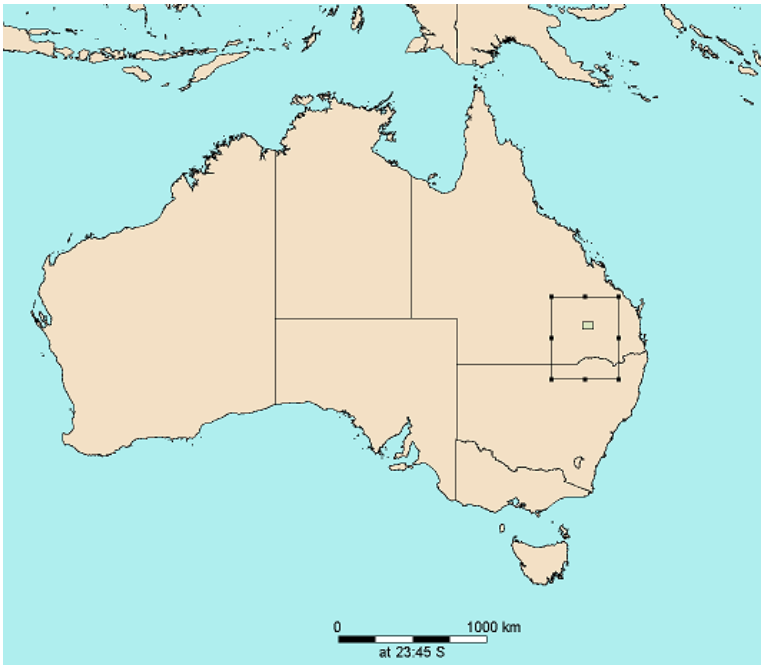

Figure 4.1: Location of the 600x430 km basin wide model (box) and 80x60 km nested model (green box).

The simulation area was chosen to include the present day Surat Basin sediment outline as well as the surrounding (palaeo)highs to realistically simulate sediment flow and deposition into the basin (figure 4.2). The south western corner of the simulation area is located at UTM coordinates 55J 52500 6675500.

The nested model is incorporated in the Basin-wide Model at the location of the EPQ-7 tenement with 55J 725000 7045500 being the coordinates of the south western corner.

The simulation area continues eastward from UTM zone 55J into UTM zone 56J. As a zone transition would unnecessarily complicate the model grid coordinate system, UTM zone 55J coordinates are used for the entire grid.

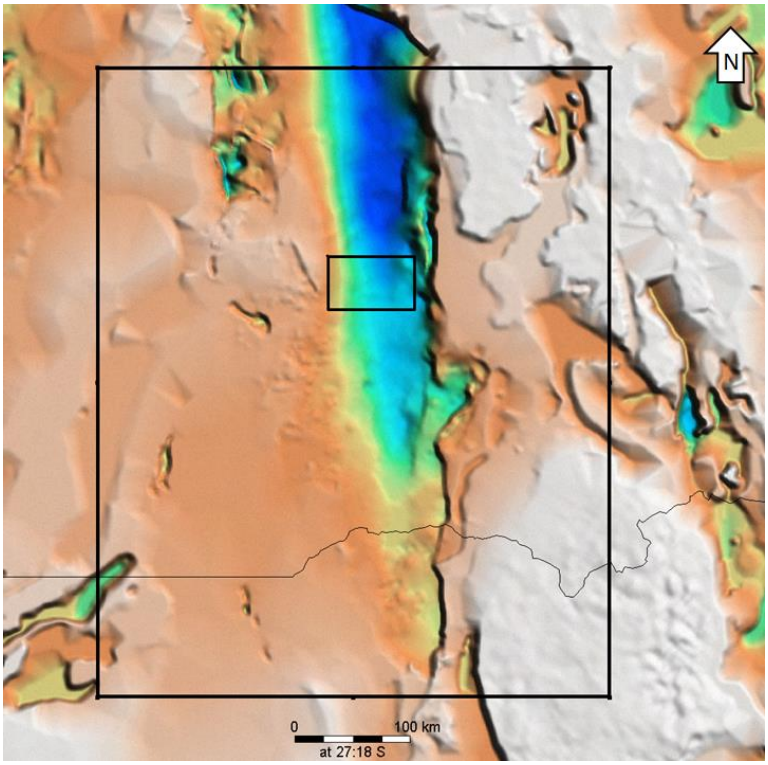

Figure 4.2: Outline of the Basin-wide Model grid (large box) and Nested Model grid (small box), superimposed on a depth to basement map, , color indicates basement depth: blue (deep) to white (shallow) (FrogTech, 2005).

4.1.2. Basement topography and tectonics

The basement topography file has the same dimensions as the model grid; it adds an elevation value to each grid node to resemble the initial basin topography at the start of simulation. On this surface, the sediment will be deposited in the model.

It is very likely that the Surat Basin topography, just before Precipice Sandstone deposition, resembled a peneplain as a result of Middle to Late Triassic uplift and erosion (Green, 1997; Korsch and Totterdell, 2009). Although peneplained, it is likely that there were some basement highs on the basin margins, as no or less Surat Basin sediment was deposited here. These elevated basement blocks are located in the southwest (St George/Bollon slope), northeast (Auburn Arch, Yarraman block) and southeast (Texas High)(see figure 2.2). Furthermore, the Nebine and Kumbarilla ridges provide a more subtle high that separated the Surat Basin from respectively the Eromanga and Clarence Moreton basins in the Early Jurassic. Using isopach maps of the Precipice, Evergreen and Hutton formations; general locations and relative elevation of basin highs were established. This was done by comparing the location of

depositional boundaries of the modelled formations as they move further onto the basement highs with each formation in isopach maps. This approach was only possible on the western, southern and south-eastern formation boundaries; here the formation boundaries represent depositional boundaries or zero-edges (Veevers et al., 1982; Elliot, 1993; Martin, 1981; Power and Devine, 1970). So here, the elevated basement blocks are included in the initial basin topography (figure 4.3).

In the north and northeast, the present day formation boundaries are erosional so do not represent the original depositional boundaries. It is likely that the Surat Basin extended beyond these boundaries at the time of deposition. Power and Devine (1970) estimated the original depositional northern depositional boundary to lie 200 km further north from the present day boundary. Exon (1976) proposed that some basement highs in the northeast were a source of Surat Basin sediments. To recreate this situation, the topography north of the erosional boundary was chosen to continue similar to the topography south of the erosional boundary and in the northeast the margins were set to have increased topography. This results in a basin shape with an open margin to the north, with higher uncertainties in the north and northeast (figure 4.3).

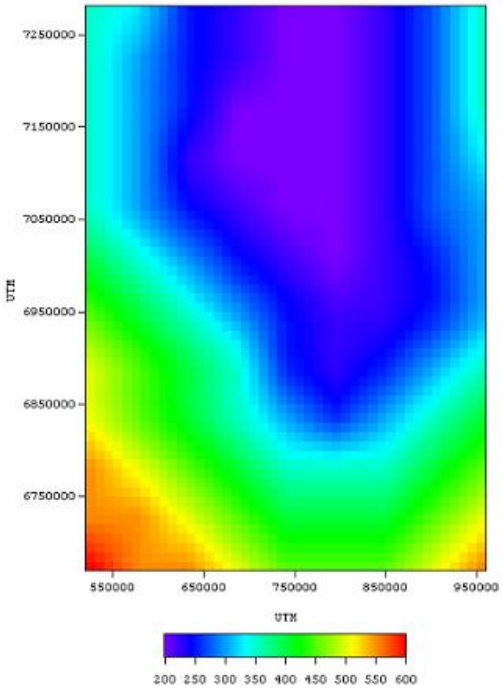

Figure 4.3: Initial topography for the Basin-wide Model in meters above base level.

The tectonics module allows Sedsim to incorporate vertical movement of the grid nodes. In order to find the subsidence for each formation, the formation thicknesses are assumed to record minimum subsidence (see figure 4.4). The thicknesses are then increased by 30% to account for sediment compaction. The thicknesses used for the Precipice and Evergreen formations are based on the study by Dixon et al. (2011), which was provided by the Geological Survey of Queensland. Dixon et al. (2011) used seismic and well data to constrain a model of important stratigraphic surfaces in the basin: base Precipice Sandstone, base Evergreen Formation, base Hutton Sandstone, top Walloon Coal Measures.

The basin-wide horizon data were cropped to the model coordinates and resampled to the model grid size. The depths of top and base of the Precipice and Evergreen formations were subtracted to find the thickness, and thus the assumed minimum subsidence at each grid node. As the top of the Hutton Formation is not separated in the study of Dixon et al. (2011), the thickness isopachs from Green et al. (1995) were used to constrain the thickness of the Hutton Formation. This was done by manually recreating the isopach in a grid at coarse resolution after which it was resampled to the appropriate model grid size. The time periods of activity were added to the subsidence values in the tectonic input file.

The subsidence rate was assumed to be constant during deposition of the Evergreen and Hutton formations. In early model iterations the sand fraction distribution of the Precipice Sandstone did not reach far enough basinward, independently of sediment flux or increased sand fraction. By increasing the subsidence rate for the early Precipice Sandstone, the depositional gradient increased, resulting in sand distribution reaching sufficiently basinward. Subsequently, half of the total Precipice Sandstone subsidence is simulated in the first quarter of the time chosen for Precipice Sandstone deposition.

4.1.3. Sediment and sediment sources

Four grain sizes were used in the model: medium sand, fine sand, silt and clay. Their respective grain diameters in mm are: 0.45, 0.15, 0.035, 0.0010. As definitive provenances are not known for the sediment of the Surat Basin, the locations of the sources in the model are based on literature describing the depositional setting, paleogeography and likely provenances (Sell et al., 1972; Exon, 1976; Green, 1997; Hoffman et al., 2009). The sediment sources in the model are located on the basin margins with a general flow direction from the basin margins to the centre (see figure 4.4).

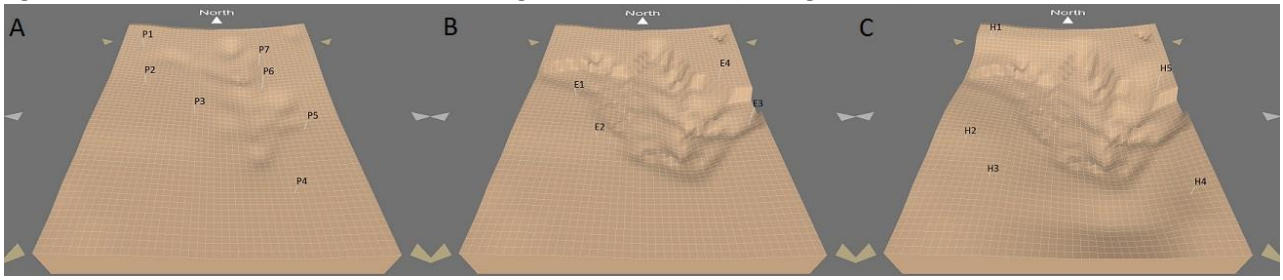

Figure 4.4: Total subsidence and locations of sediment sources at the end of the depositional episode of: (A) the Precipice Sandstone, (B) Evergreen Formation and (C) Hutton Sandstone.

To recreate the large-scale sediment heterogeneity found in the Surat Basin, the sediment sources are set to switch between active and inactive states several times during the deposition of a formation. This results in large-scale changes in flow direction and introduces more heterogeneity in the facies distribution. The active time period of a source is divided into smaller time periods of 50 k years. In each of these periods the source has a partly random location and discharge. The discharge is allowed to randomly vary within 40% above and below the set value, although the total discharge per depositional episode of a formation is kept roughly constant in order to maintain similar total sediment volumes in the model. The location of a source is allowed to randomly vary within 25 km in the north-south direction and 12.5 km in the east-west direction from the initial chosen location. The changing north-south location moves the source roughly perpendicular to the general flow direction, resulting in a more

pronounced effect on the sediment distribution. The partly random discharge and location of sources result in small-scale heterogeneity within the facies distribution at a high temporal resolution.

In Sedsim, the maximum slope parameters define the maximum depositional slope the sediment can attain. The following slope parameters (dx/dy) were used in the model:

	Medium sand	Fine sand	Silt	Clay
Above sea-level	0.007	0.0055	0.005	0.0004
Below sea-level	0.0006	0.0004	0.0003	0.0002
Reworked below sea level	0.005	0.004	0.003	0.0002

Table 4.1: Maximum depositional slope parameters

4.1.4. Sea-level

The sea-level module uses a text input file to specify the sea level in meters above or below base level at a given time in the simulation. As the Jurassic Surat Basin depositional environment is dominantly of a fluvial and lacustrine nature, the sea level in the simulation represents the lake level in the Surat Basin. The Precipice and Hutton formations are deposited in varying fluvial environments with little to no lacustrine influences. At these times the model lake levels are set to values that lower the water level below the elevation at which sediment deposition occurs and thus the depositional environment remains fluvial.

Contrary to the Precipice and Hutton sandstones, the Evergreen Formation has experienced significant lacustrine influences during deposition. Based on the literature, the Lower Evergreen Formation depositional environment in the model is assumed to consist of high and lower energy streams interacting with freshwater lakes. The Boxvale Sandstone Member is assumed to be deposited by both high energy streams and lacustrine shoreline deposits in lakes with migrating shorelines. The Upper Evergreen Formation with the Westgrove Ironstone Member is assumed to resemble a low energy environment at a time of maximum flooding.

Based on the above descriptions it is assumed that during Evergreen Formation deposition, lake levels rose steadily with a maximum during Late Evergreen Formation deposition. The rising lake levels were set to fluctuate, to simulate sediment reworking by migrating shorelines, specifically in the Boxvale Sandstone. The fluctuation consist of large 0.5–1 Ma fluctuations and smaller 0.1 Ma fluctuations, the smaller scale fluctuations are generated by allowing the values to randomly vary within 10 meters from the set value (figure 4.5). It is not known whether the lake was one large discrete lake or a number of lakes. In the simulation it is assumed to be a single large lake.

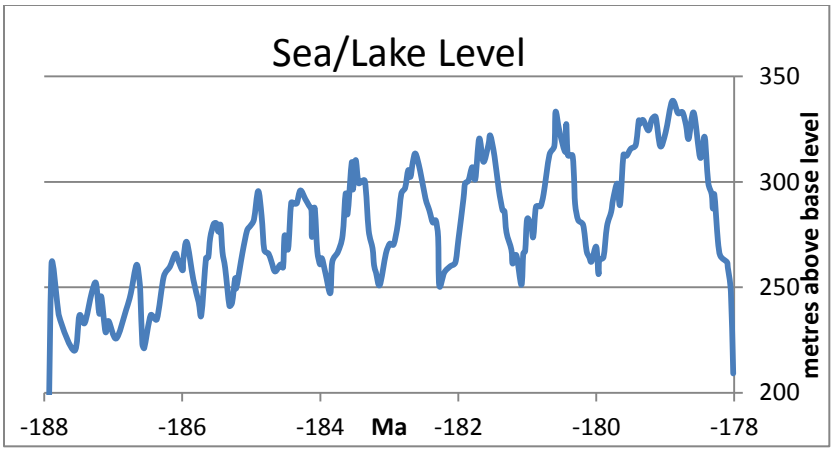

Figure 4.5: Sea/lake level curve at the time of Evergreen Formation deposition.

4.1.5. Porosity and compaction

In Sedsim compaction occurs by means of porosity reduction and is calculated using a look-up table containing porosity values for different fine-to-coarse ratios as a function of effective stress, which is the vertical compressive stress minus the fluid pressure (Terzaghi, 1936; Terzaghi and Peck, 1948). As the effective stress increases with burial during a simulation, the porosity corresponding to the effective stress and fine-to-coarse ratio is selected from the look-up-table (see table 4.2). The four siliciclastic grain sizes are classified as either fine or coarse sediment in the fine to coarse used in the lookup table. In the model, the medium and fine sand grain sizes are classified as coarse sediment and the silt and clay grain sizes are classified as fine sediment. Sedsim automatically interpolates porosity values between the given effective pressures of the look-up-table. For each kilometre of burial the effective stress is assumed to increase by 22.5 MPa. In the lookup table five effective pressures, resembling burial depths, and 12 different fine-to-coarse ratios were used to reduce the porosity with burial to simulate syn-depositional and post-depositional compaction.

The porosity-depth data for the Surat Basin from the QCGI (2009) and Bradshaw (2009) yield no apparent porosity-depth relation suitable as a basis for the Sedsim porosity look-up-table. Furthermore, the present day sediment depths are unlikely to represent the maximum burial depths due to extensive Cretaceous uplift and exhumation. Instead, sandstone and shale porosity-depth relations used by Sclater and Christie (1980) and Gluyas and Cade (1997) were used to guide the porosity look-up table in the model.

Overburden → F/C ratio ↓	Overburden: 0 m (0 Mpa)	500 m (11.25 Mpa)	1500 m (33.75 Mpa)	3000 m (67.5 Mpa)	5000 m (112.5 Mpa)
0	0.48	0.42	0.32	0.23	0.17
0.05	0.47	0.4	0.3	0.21	0.16
0.1	0.43	0.38	0.28	0.18	0.14
0.15	0.41	0.35	0.25	0.16	0.12
0.2	0.39	0.33	0.23	0.14	0.11
0.25	0.37	0.3	0.2	0.12	0.1
0.3	0.35	0.27	0.17	0.11	0.09
0.4	0.32	0.24	0.15	0.1	0.09
0.5	0.38	0.23	0.14	0.1	0.08
0.65	0.45	0.25	0.16	0.11	0.07
0.85	0.55	0.29	0.18	0.1	0.05
1	0.65	0.3	0.13	0.06	0.03

Table 4.2: Porosity look-up table.

To incorporate post-depositional compaction into the model, the maximum burial depth needed to be known. The maximum burial depth for the Surat Basin consists of the current burial depth plus an estimate of the section lost to erosion during the Cretaceous to present. Gallagher (1994) estimated the eastern and western margins of the Surat Basin to have lost respectively 2.5 km and 1 km. Reza et al. (2009) estimated erosion in the Taroom Trough, roughly the middle of the Surat Basin, to be 1.5 km. Marshallsea (1985) reported a denudation of 3 km, north of Surat Basin. From these estimates 1.5 km was used in the model, as the wells used in the study of Reza et al. (2009) are located centrally in the simulation area and 1.5 km corresponds roughly with the estimates of Gallagher (1994).

Using this 1.5km as section lost and the present day depth to the base of the Surat Basin of roughly 2.5 km at the basin centre, the maximum burial depth would be 4 km to the base of the Precipice Sandstone. The 4 km minus the total model sediment thickness of 550 meters at the centre, result in a maximum burial of 3.45 km onto the top of the Hutton Sandstone. For model simplicity, the maximum burial is assumed to be constant for the entire basin in the model.

4.2. Model-to-well comparison

Sedsim can generate output data for single or multiple grid nodes, containing information such as: sediment layer depth, grain sizes, deposition type, porosity and water depth. This information can be used to generate wells, or pseudo-wells, of the Sedsim model. These pseudo-wells can be compared to real wells, referred to as model-to-well comparisons.

In total, eight wells have been used in the model-to-well comparisons: Kinkabilla Creek-1, Haricot-1, North Cherwondah-1, Bentley-1, Taroom-15, Teatree-1, Pineview-1, Arlington-1. The wells are located throughout the basin (figure 4.6). Pineview-1 and North Charwondah-1 are located in the potential CO_2 storage tenement EPQ-7. Arlington-1, Bentley-1 and Teatree-1 are located in what is considered the basin centre, south of EPQ-7. Haricot-1 is located near the basin margin the northwest and Kinkabilla Creek-1 is located on the St. George slope, somewhat west of the basin centre.

The grid node closest to the location of a given well was used to generate the model pseudo-well data. Sedsim can automatically select the grid node closest to a well location. The grid nodes are rarely located at exactly the same location as the actual well, but the 10x10 km grid spacing ensures that the grid nodes are always less than 7 km ($\sqrt{(5^2+5^2)}$) removed from the actual well location. The large size of the basin and sediment continuity over such a relative short distance, make the offset negligible.

Figure 4.6: Locations of the wells used in the well comparisons, grid cells have 10x10 km dimensions.

From the eight wells, the gamma ray logs and well data derived porosity are compared to the model pseudo-well data. To do this effectively, the pseudo-wells need to be displayed in the same depth interval as the wells. The base of the pseudo-well data was given the same depth as the base of the Precipice Sandstone in the corresponding wells, and for each simulated sediment layer the thickness was added to this depth.

4.2.1. Pseudo-gamma ray comparisons

As Sedsim does not generate gamma ray values of the sediment, model data needs to be transformed into pseudo-gamma ray values. This is done by two pseudo-gamma ray transforms, one based on the relative grain size abundances in a model sediment layer and one based on the thickness of the sediment layer. The pseudo gamma ray values from both transforms are then combined into a single pseudo-gamma ray value on a 50/50 basis (see figure 4.7).

Sedsim output data specifies each grain size in meters per layer of sediment. This value, for each of the four grain sizes, is divided by the sum of all grain sizes and multiplied by the gamma ray value chosen for

the specific grain size. This way a pseudo-gamma ray value is given to a layer based on the relative grain size abundances:

$$pseudo\ GR = \frac{G_1}{G_1+G_2+G_3+G_4} * GR_1 + \frac{G_2}{G_1+G_2+G_3+G_4} * GR_2 + \frac{G_3}{G_1+G_2+G_3+G_4} * GR_3 + \frac{G_4}{G_1+G_2+G_3+G_4} * GR_4$$

For medium sands (G_1) the pseudo-gamma ray (GR_1) was set to 20 API, for fine sand (G_2) 40 API (GR_2), for silt (G_3) 85 API (GR_3) and for clay (G_4) 125 API(GR_4). The gamma ray logs of the wells used all tend to have slightly different values for roughly similar sediment, probably caused by differences in measuring equipment or processing. That is why the pseudo gamma ray values given above might not match the well data exactly, but the data can still be compared despite a possible offset.

It is assumed that, in reality, thin sediment layers generally result in high gamma ray values as they often represent shale or silt layers deposited in low energy or sediment starved environments. Furthermore, silt and shale layers tend to be thinner as they compact more than sandstone layers during burial. The same can be seen in the Sedsim simulation. Furthermore, the fine-grained sediment is mainly deposited away from the sources where the energy is low, as the sediment moves away from the source, the area covered by the sediment increases, resulting in thinner fine-grained layers with increasing distance from the sources.

To incorporate the effect of layer thicknesses on the pseudo gamma ray values, each sediment layer has the precise thickness calculated from the top and bottom depth from the Sedsim data. The layer thickness is divided by the maximum thickness found in the interval, a 1 represents the thickest layer and a 0 represents the thinnest layer. The maximum gamma ray value is reduced by this relative thickness and multiplied by the difference between the maximum and minimum gamma ray values. The thickest layer will now result in a minimum pseudo-gamma ray value and the thinnest layer in a maximum pseudo-gamma ray value:

$$pseudo\ GR = max.GR - \frac{layer\ thickness}{max.layer\ thickness}(max.GR - min.GR)$$

Minimum (min.GR) and maximum (max.GR) pseudo gamma ray values are respectively 20 and 125 API, similar to the relative grain size transform.

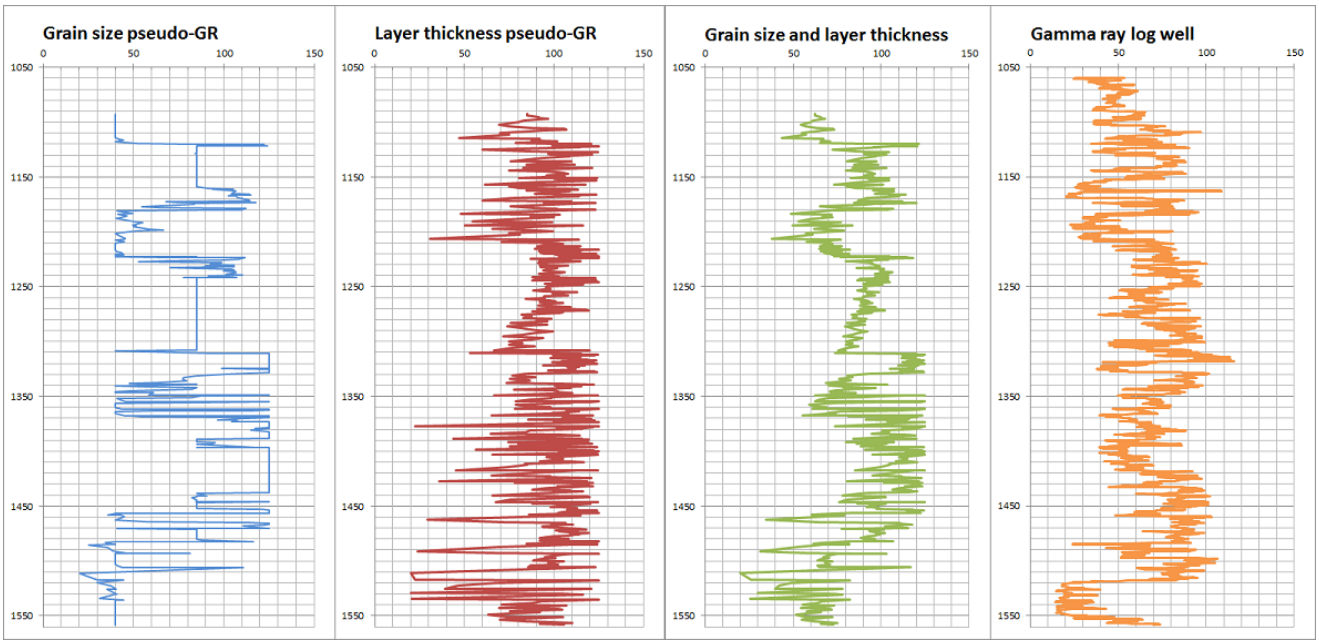

Figure 4.7: Relative grain size abundance related pseudo-gamma ray log (blue), layer thickness related pseudo-gamma ray log (red), 50/50 combination (green) and the gamma ray log of the well (orange).

4.2.2. Porosity model-to-well comparisons

For porosity model-to-well model comparisons (figure 4.8), the effective porosity was calculated for the wells and plotted together with the model porosity against depth. Sedsim porosity data are directly available in the pseudo-well output data. For the well log-derived porosity, neutron porosity and bulk density wireline logs had to be available. Porosity based on sonic logs proved problematic in non-sand intervals.

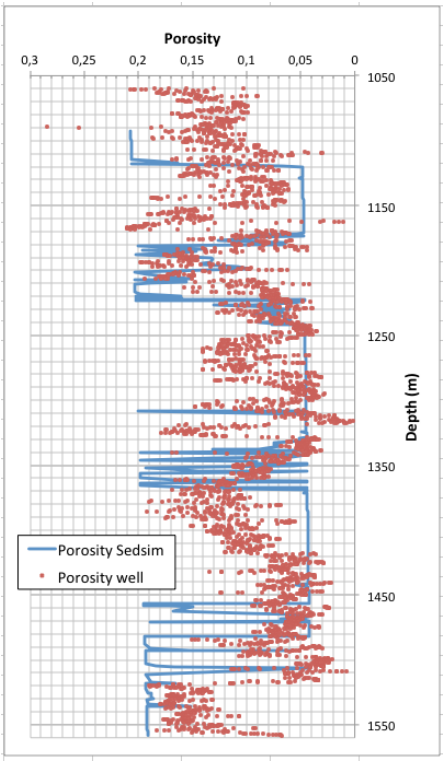

Figure 4.8: Model-to well porosity comparison.

The effective porosity (ϕ_E) is calculated using the density derived porosity (ϕ_D), apparent neutron porosity (ϕ_N) and shale volume fraction (V_{shale}). The density derived total porosity or fraction of the bulk rock volume that is fluid filled was calculated using the bulk density log data:

$$\phi_D = \frac{(\rho_{ma} - \rho_b)}{(\rho_{ma} - \rho_{fl})}$$

With ρ_{ma} = matrix density: 2.65 g/cm^3 (sandstone), ρ_b = bulk density log value, ρ_{fl} = fluid density: 1 g/cm^3.

The apparent neutron porosity (ϕ_N) is found by adding 0.04 to the neutron porosity log values to correct the log from apparent limestone porosity to apparent sandstone porosity. Using the apparent neutron porosity, the total porosity from the average neutron and density porosity (ϕ_A) is calculated:

$$\phi_A = \frac{(\phi_D + \phi_N)}{2}$$

In order to distinguish the shale or clay volume relative to the sand volume, the shale volume fraction was calculated using:

$$V_{shale} = \frac{(GR_{log} - GR_{min})}{(GR_{max} - GR_{min})}$$

With GR_{log}= gamma ray log value, GR_{min}= minimum gamma ray log value corresponding with a clean sandstone interval, GR_{max}= maximum gamma ray log value corresponding with a shale or clay interval.

The effective porosity (ϕ_E) is the average neutron and density porosity (ϕ_A) minus the pore space fraction that is occupied by shale or clay (V_{shale}):

$$\phi_E = (1 - V_{shale})\phi_A$$

Alternatively, the effective porosity can also be calculated using only the bulk density derived porosity instead of including the average neutron and density porosity. The combination of both resulted in a less erroneous result and generally, if the bulk density was logged, the neutron density was logged as well.

4.3. Tuning process

In the tuning of the Initial Model, the objective was to roughly tune the formation thicknesses and sediment heterogeneity to the cross-sections of the Surat Basin included in the QCGI (2009) report. These cross-sections show several wells on various transects through the basin. The gamma ray logs shown here give a good idea of the general sediment character (sand or mud dominated) and heterogeneity for the model to match. The comparison between the cross-sections and the model was done visually by selecting the nearest cross-section (fence) through the Initial Model in the Sedview visualisation. This is not a very accurate method, and only a rough match could be achieved. The thickness of the sediment formations in the model were compared to thickness maps generated for the subsidence, based on Dixon et al. (2011) and isopach maps from Green (1997).

The higher grid node density of the Basin-wide Model enabled direct comparisons between wells and model generated pseudo wells. For each well location, the model pseudo-gamma ray logs were compared to the well gamma ray logs. For four well locations well log based porosity was compared to the model porosity. During the model-to-well comparison tuning process, the goal was to have matching formation boundary depths and roughly matching gamma ray signals. Priority was given to the inclusion of important large-scale features from the well logs into the model. Features such as the transition from the sandy Lower Precipice Sandstone to the more muddy Upper Precipice Sandstone or the location and depth of the Boxvale Sandstone within the Evergreen Formation. The Hutton Sandstone was given a lower priority as it plays a less significant role in the Precipice/Evergreen geostorage play, although the Hutton Sandstone ensures accurate overburden for early compaction in the model.

At the start of the tuning process a good model-to-well match was attempted for all the wells used. This proved to be impossible, as adjustments to improve the match in the basin centre would often reduce the match on the basin margins. As the main area of interest is the potential CO_2 storage site at the EPG-7 tenement, it became the focal point of the tuning process. At his stage, the Arlington-1 well was included in order to improve well coverage in the basin centre. The Pineview-1 well was introduced at a later stage, to test the match in the EPQ-7 tenement, and to do final fine-tuning.

In the tuning process, most adjustments to the model were done using the sediment input parameters, as formation thicknesses, depths of formation tops, pulses of increased coarse grained sediment, or a fine grained interval, are all directly influenced by modifying the sediment input parameters. The total discharge of sources into the model during the deposition of a formation will change the formation thickness and depth of the top. Local variations in thickness can be addressed by the discharge in the

most proximal sources. The grain size distribution is represented by the pseudo-gamma ray log and is largely influenced by the sediment fractions present in the sources but also by source locations and discharge volumes. To tune the simulation in an efficient manner the sediment source input files were set up per formation in Microsoft Excel to allow quick and easy changes. Around 45 Basin-wide Model iterations were used in the tuning process. For each model iteration, a change was made to improve the match with the wells. No tuning was done on the Nested Model of the EPQ-7 tenement, as it is an interpolation within the Basin-wide Model with a higher data density.

4.4. Permeability Model

Sedsim can export the model data in the Eclipse format (*.grdcl), which can be used in a wide range of modelling software. To create a permeability model using the Sedsim model, the model Eclipse files are imported into the Roxar RMS reservoir modelling software. Here, the Sedsim model porosity data is used to calculate the vertical and horizontal permeability with a porosity-permeability transform. Furthermore, RMS was used to generate statistical information and representations of the Surat Basin stratigraphic forward model.

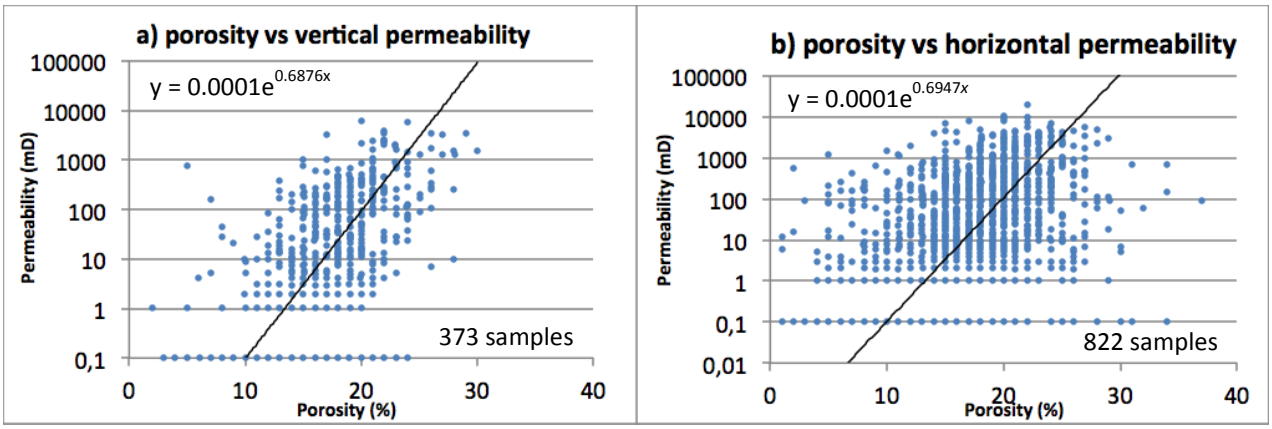

Figure 4.9: Precipice Sandstone porosity plotted versus vertical (a) and horizontal (b) permeability including the trend line used for the porosity-permeability transform, data from QCGI (2009)

To find the porosity-permeability transforms, the porosity-permeability plots from QCGI (2009) were digitized using the Graphclick software program, and imported to Microsoft Excel. Here, an exponential trend line was plotted to best fit the porosity-permeability plots of each formation (figure 4.9). The trend lines initially did not match the vertical trend of data, this was corrected by setting the trend lines to intercept the Y-axis at 0.0001. As a result, no R^2-value can be calculated. The trend line equations were used as porosity-permeability transform, for both the horizontal and vertical permeability of each of the modelled formations. Table 4.3 and figure 4.10 show the porosity-permeability relations found.

Formation	Vertical porosity-permeability transform (No. of samples)	Horizontal porosity- permeability transform (No. of samples)
Precipice Sandstone	$0.0001e^{0.6876\phi}$ (373)	$0.0001e^{0.6947\phi}$ (822)
Evergreen	$0.0001e^{0.7936\phi}$ (27)	$0.0001e^{0.6605\phi}$ (816)
Hutton Sandstone	$0.0001e^{0.4955\phi}$ (10)	$0.0001e^{0.5483\phi}$ (34)

Table 4.3: Porosity-permeability transforms found for the modelled formations of the Surat Basin.

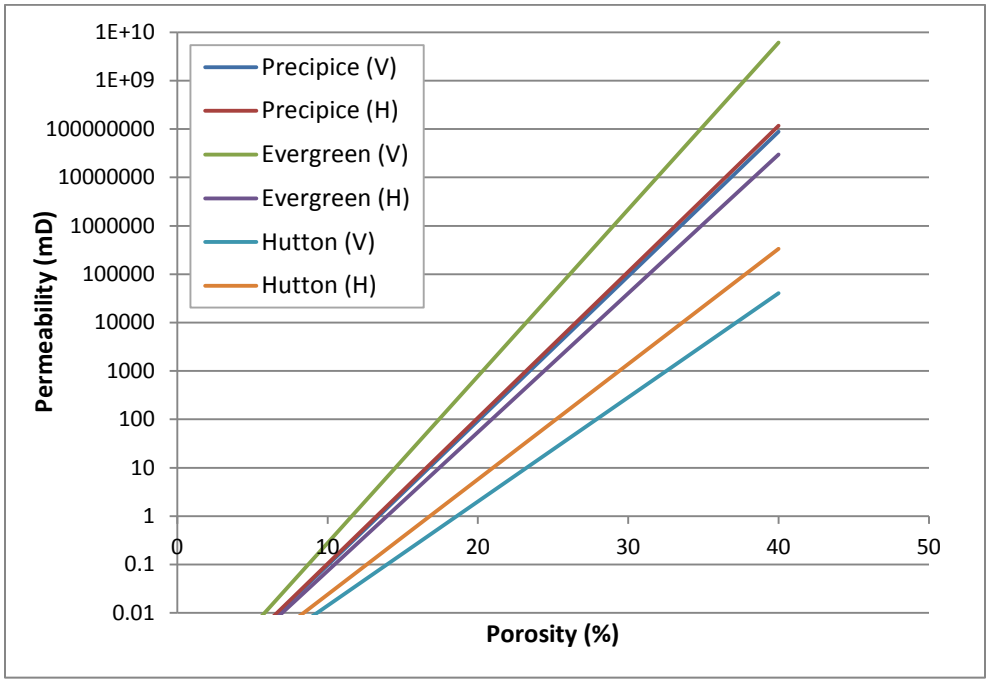

Figure 4.10: Porosity-permeability relations found for the modelled formations, for both the vertical (V) and horizontal (H) permeability.

5. Results

The main result of the study is the stratigraphic forward model of the Surat Basin, created with the Sedsim stratigraphic forward modelling package. The model covers most of the Surat Basin, with a simulation area of 640x440 km with 10 km grid spacing (figure 5.1). For the EPQ-7 potential CO_2 sequestration tenement, an 80X60km 1km grid spacing nested model was built (figure 5.2). In these models the deposition of the Early Jurassic Surat Basin sediment succession is simulated, from Precipice Sandstone (202 Ma) to Hutton Sandstone (166 Ma) (see figure 5.3,5.4,5.5). The Surat Basin stratigraphic forward model can provide data such as: grain size distribution, porosity, net-to-gross and permeability. The potential value of the Surat Basin stratigraphic forward model generated data, depends on the degree to which the model data matches subsurface data of the basin. In this context, the results of the tuning process can be considered additional results.

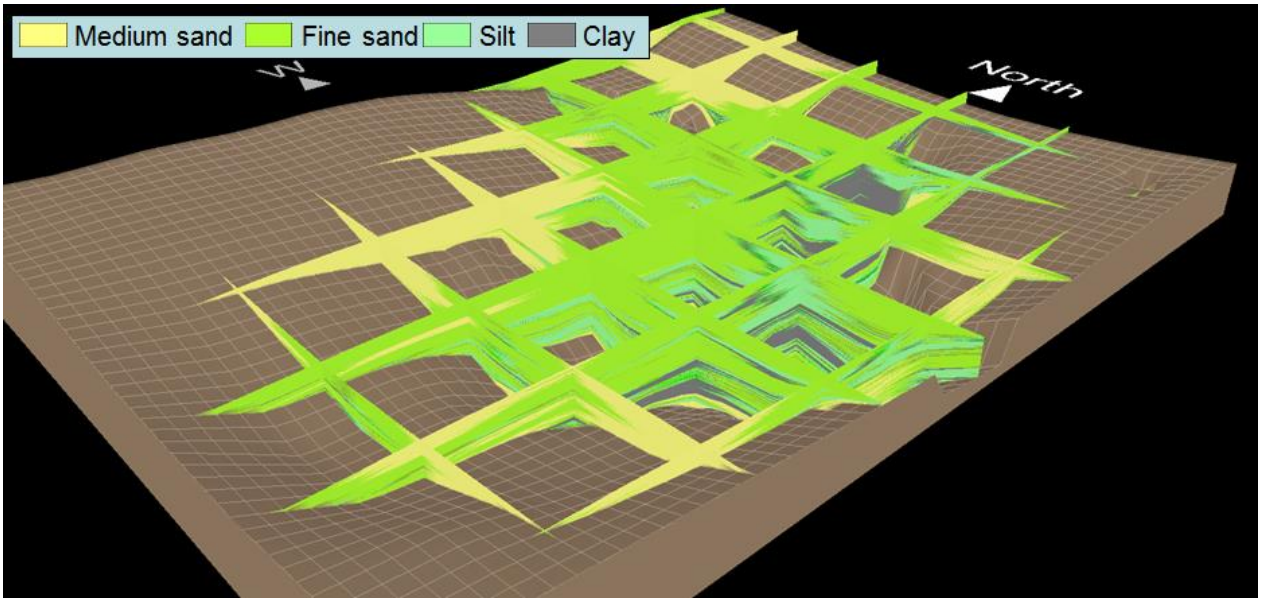

Figure 5.1: The Basin-wide model with every eighth fence turned on at 100x vertical exaggeration and 10x10 km grid cells.

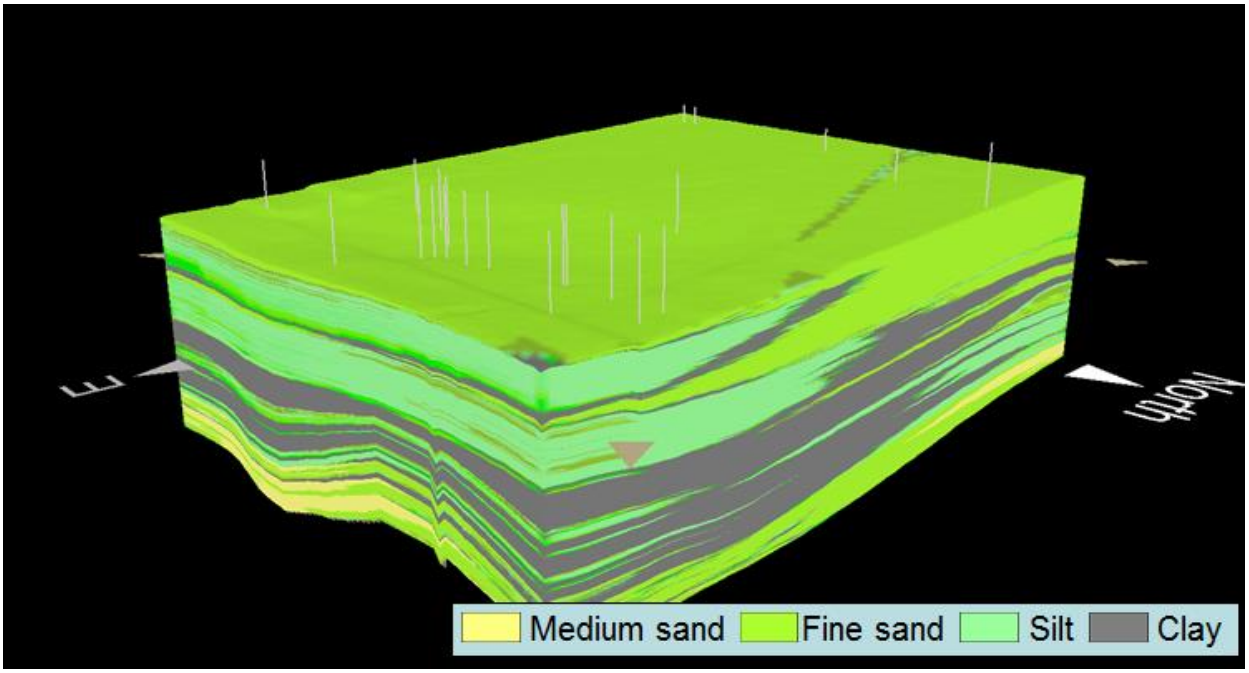

Figure 5.2: The Nested Model with the complete sediment volume turned on at 60x vertical exaggeration.

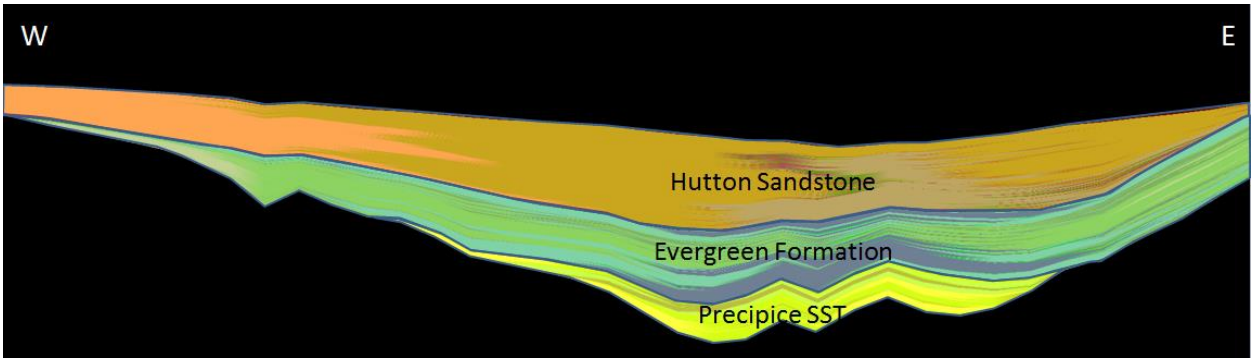

Figure 5.3: Cross-section through the model from the St. George slope in the west, to the Kumbarilla Ridge in the east at 100x vertical exaggeration over a distance of 380 km.

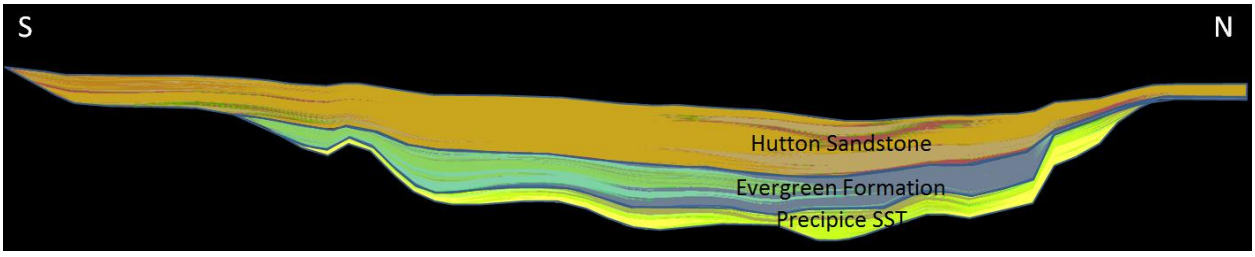

Figure 5.4: Cross-section trough the model along the Mimosa Syncline at 100x vertical exaggeration over a distance of 600 km.

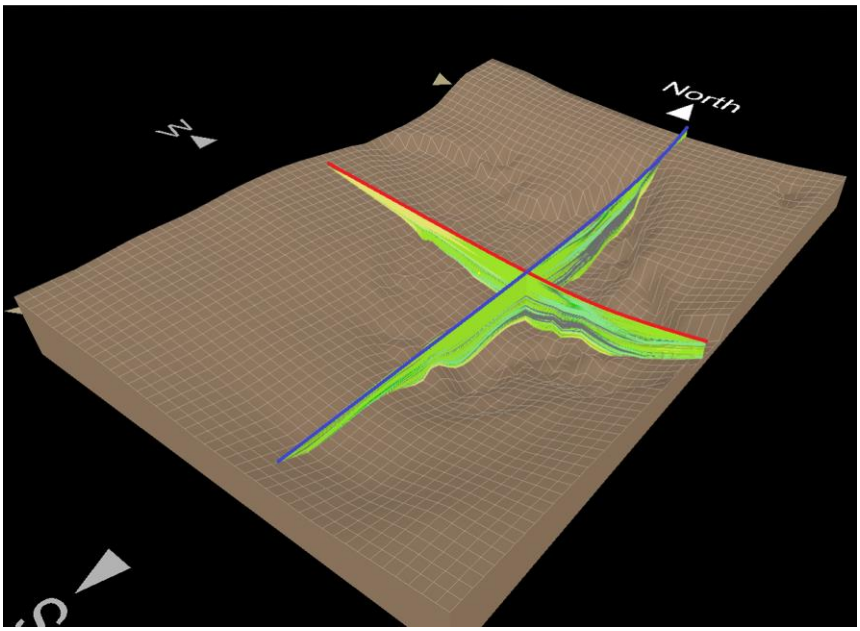

Figure 5.5: Locations of the cross-sections in figures 5.3 (red) and 5.4 (blue).

5.1. Porosity

The porosity in the model ranges from 3.7% to 24%, with a bimodal distribution. Most values are close to either the minimum or maximum values, some mid-range porosity values (10-17.5%) are almost non-existent (figure 5.6).

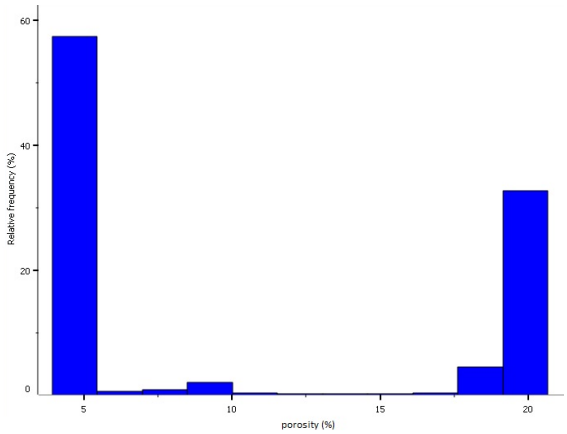

Figure 5.6: Porosity relative frequency distribution

Despite the bimodal distribution, pseudo-well porosity of the Precipice Sandstone and Evergreen Formation seem to largely plot in the value range of the well data, and at some intervals seem to follow the porosity trend of the wells (figure 5.7). Furthermore, the vertical proportion curves clearly resemble the characteristics of the modelled formations, high porosities for the Precipice and Hutton Sandstone and largely low porosities with high porosity beds for the Evergreen Formation and its Boxvale

Sandstone Member (figure 5.8). Compared to the Basin-wide Model, the EPQ-7 nested model shows more extensive low porosity intervals (figure 5.9).

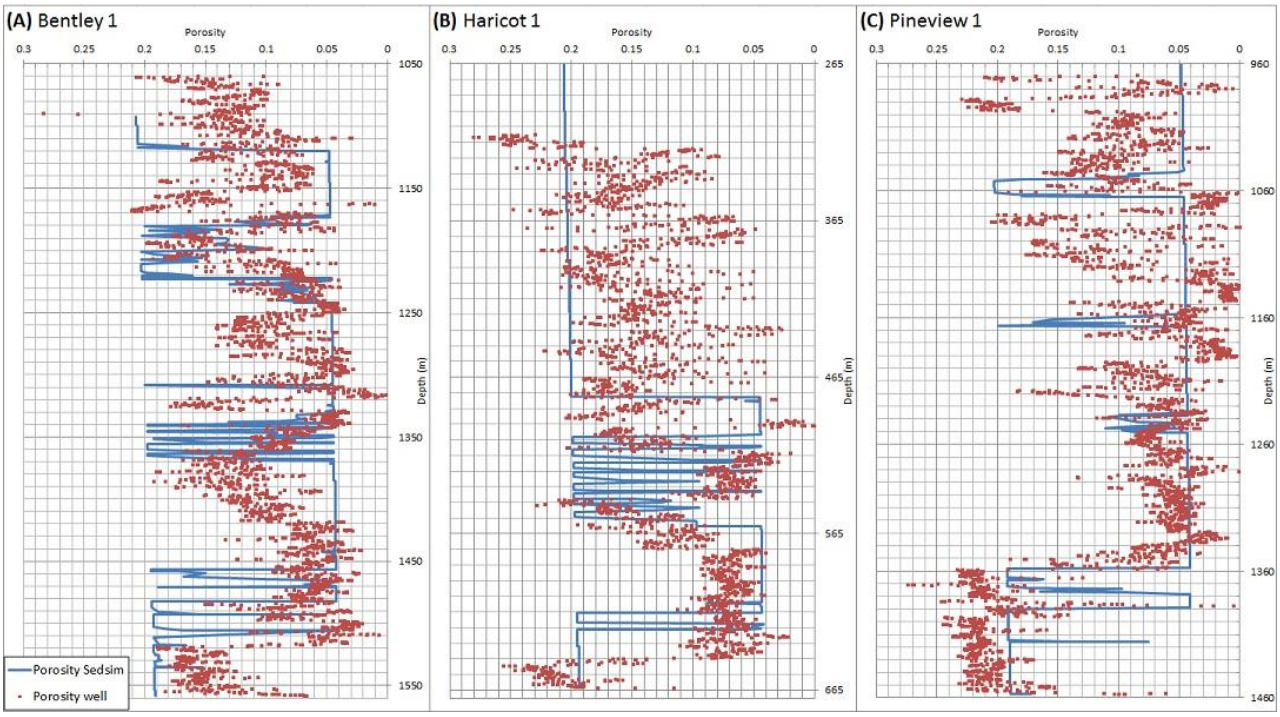

Figure 5.7: Model pseudo-well porosity and well porosity plots.

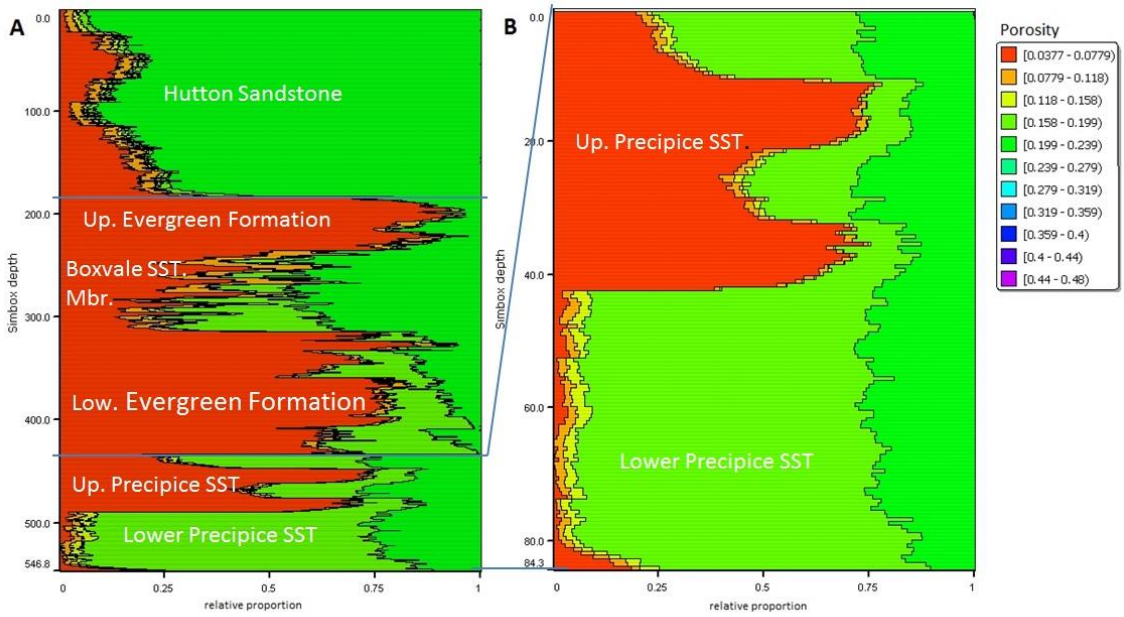

Figure 5.8: Vertical porosity proportion plots of the Basin-wide Model for the entire modelled interval (A) and the Precipice Sandstone (B).

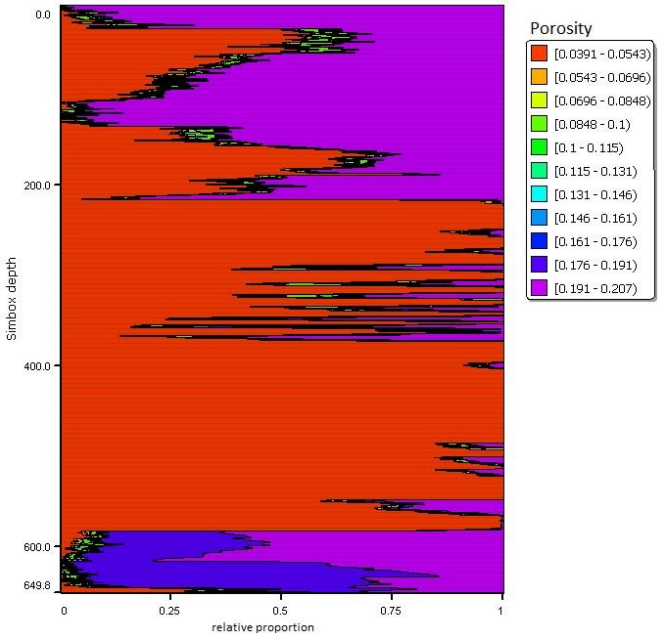

Figure 5.9: Vertical porosity proportion plots of the Nested Model

5.2. Permeability

From the porosity data, the horizontal and vertical permeability were calculated for the Nested Model (Figure 5.10), using a porosity-permeability transform. With the porosity-permeability transform for the Precipice Sandstone the values range from 0 to 172 mDarcy horizontal permeability and 0 to 149 mDarcy for the vertical permeability, with mean values of 32 and 37 mDarcy respectively. Bradshaw et al. (2009) have found highly variable permeability values for the Precipice Sandstone, with maximum values of several Darcy and a median value of 6.4 mDarcy. The permeability model does not match the maximum values found by Bradshaw (2009), although more than half of the permeability values found by Bradshaw et al. (2009) lie within in the permeability range of the model.

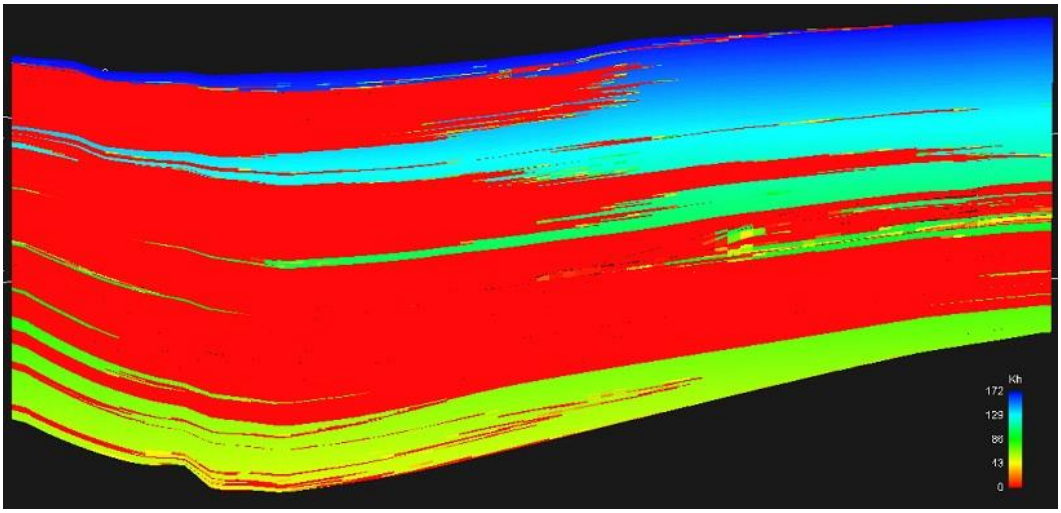

Figure 5.10: Cross-section (E-W) of the Nested Model showing the horizontal permeability.

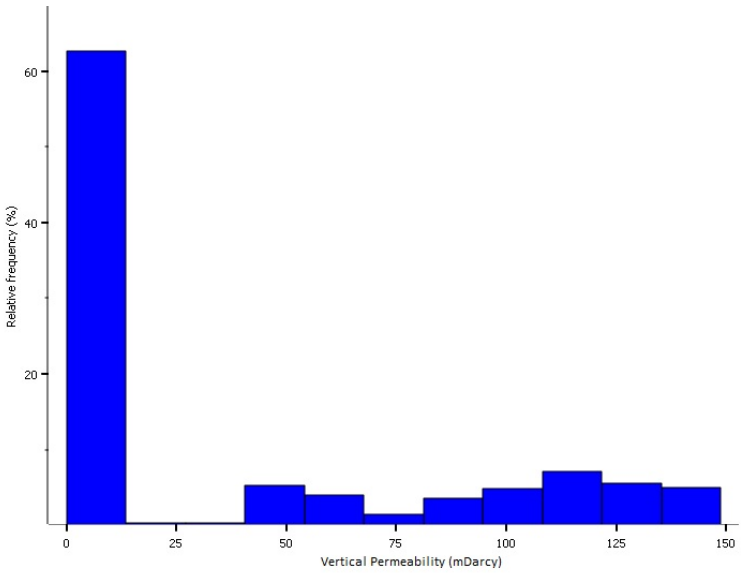

Figure 5.11: Permeability distribution.

Because the porosity–permeability transform used is an exponential function, small differences in the higher porosity values are accentuated. This results in a larger spread of the corresponding permeability values (figure 5.11). The lowest porosity values, around 3.7%, result in 10^{-3} mDarcy permeability values, these are rounded to 0 mDarcy by RMS. This causes the large amount of 0 values in the permeability distribution (figure 5.11).

5.3. Net-to-gross

The net-to-gross plots, or sand fraction plots, of the model, clearly show the positions of the sediment sources, because of the high sand fractions close to the sources. The Precipice Sandstone net-to-gross maps show sand fractions of more than 50% in most of the basin (figure 5.12A) while the Evergreen Formation is characterized by sand fractions less than 30% in the basin centre (figure 5.12C). The sand bodies of the Evergreen Formation have a more isolated character. The interaction and reworking of these Evergreen Formation sand bodies with the shores of the lake during deposition, clearly introduce a degree of sediment mixing not present in the entirely fluvial Precipice and Hutton sandstones (figure 5.13C).

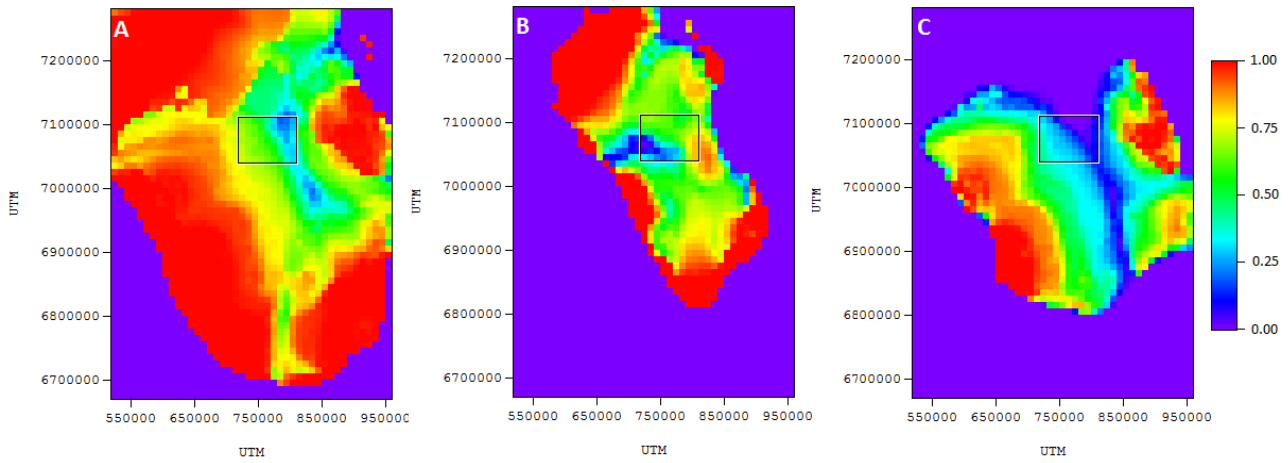

Figure 5.12: Basin-wide Model net-to-gross maps of the complete modelled sediment succession (A), Precipice Sandstone (B) and Evergreen Formation (C).

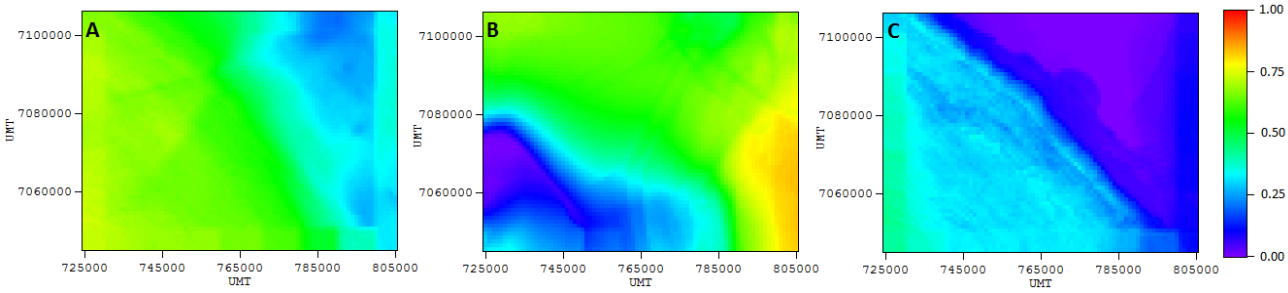

Figure 5.13: Nested Model net-to-gross maps of the complete modelled sediment succession(A), Precipice Sandstone (B) and Evergreen Formation (C).

5.4. Tuning results

Gamma ray logs from wells throughout the Surat Basin were used to tune the model, resulting in a generally good model-to-well match, especially in the basin centre and the EPQ-7 tenement (figure 5.14ABCDE). Here the pseudo-well data trend is largely similar to the trend of the well data, the general characters of the simulated formations are largely similar to the well. Wells located more distal to the basin centre have a reduced model-to-well match (figure 5.14FGH).

In order to have good matching model pseudo-gamma ray and well gamma ray plots, the thickness of the formations had to be similar. Thickness maps generated from the simulated Precipice Sandstone and Evergreen Formation show very similar formation thicknesses and location of depocentres to the thickness maps generated from seismic and well data (Dixon et al., 2011) (figure 5.15).

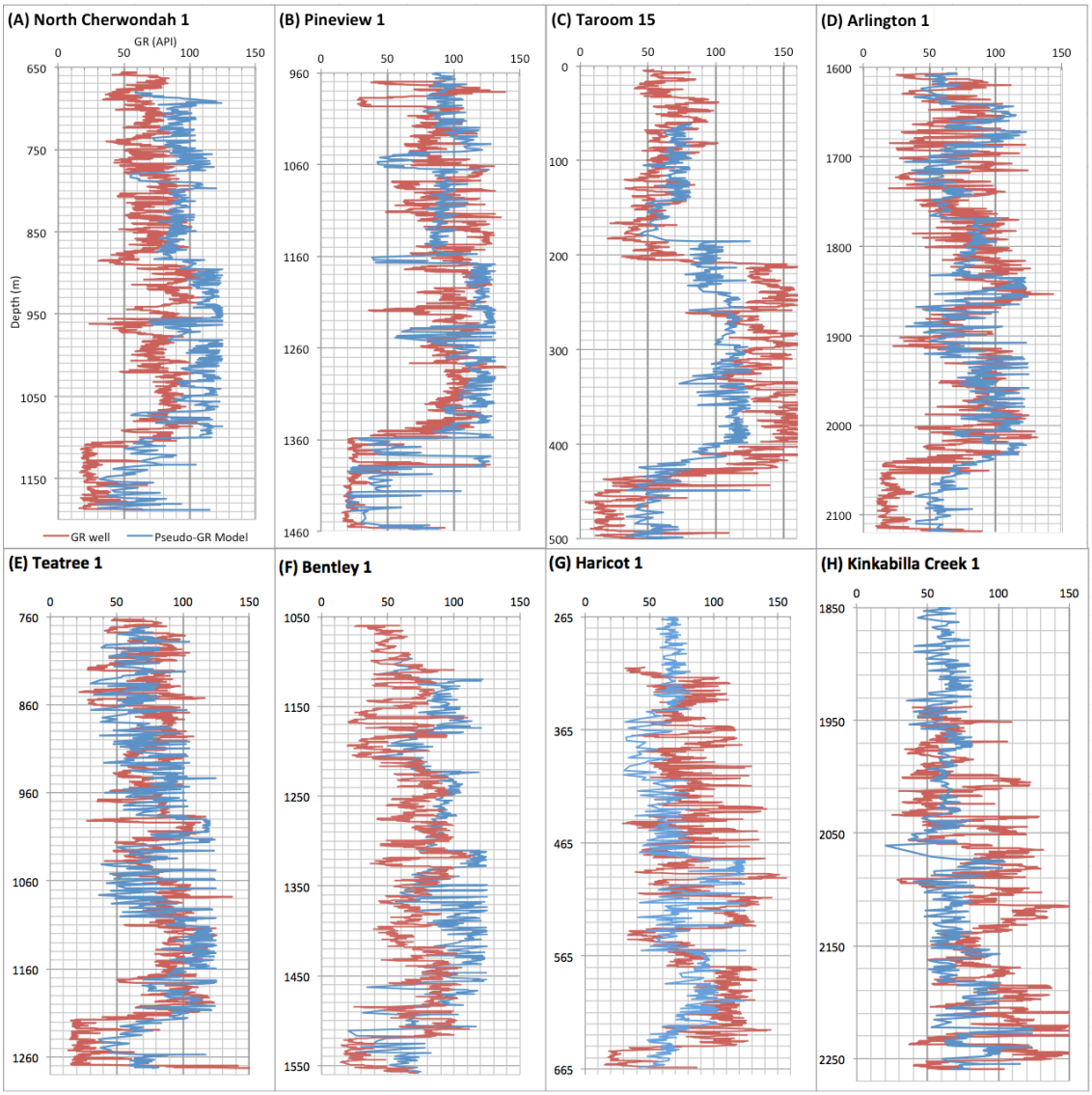

Figure 5.14: Gamma ray logs from wells (red) and model pseudo-gamma ray logs (blue).

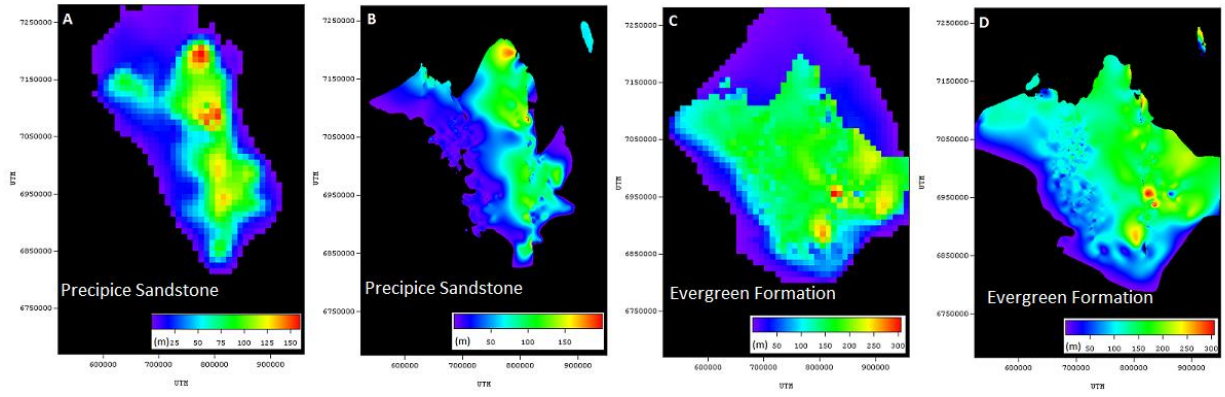

Figure 5.15: Thickness map of the Precipice Sandstone and Evergreen Formation generated from model data (A,B) and subsurface data (B,D) (Dixon et al., 2011).

6. Discussion

6.1. Model validity and improvements.

6.1.1. Model validity

Due to the inability to tune the entire basin to well data, the model is selectively tuned to the basin centre and the therein located EPQ-7 tenement. This is where the model returns the best match with the well data and can be considered a credible model for the subsurface. Towards the basin margins, the match with well data gradually reduces. Beyond the present day erosional boundaries, roughly in the north and northwest of the basin, no subsidence was included in the model, simply because no sediment was preserved in these areas. As a result, no concrete data exists to base the subsidence files upon. Thus, the model cannot be considered valid in these areas. Although it would have been possible to create a model with interpreted values for these areas, it is quite likely this will introduce more uncertainty into the model than it solves.

6.1.2. Grain size mixing and porosity distribution

The limited grain size mixing is considered the likely cause of the bimodal nature of the porosity distribution, since the mixing of the sand and non-sand grain sizes define which row in the porosity lookup table is used. The sediment deposited by dominant fluvial conditions tends to deposit in rings of similar grain size, decreasing in grain size steps with distance from the source. Although this is true for most of the model, sediment mixing did occur at the boundaries of these depositional rings, as well as at the locations influenced by the lacustrine conditions during Evergreen Formation deposition. Here, interaction of sediment with the standing water, such as the prograding nature of the Boxvale Sandstone, together with the reworking of the sediment by the rise and fall of the lake level resulted in significant grain size mixing.

A potential way to improve the grain size mixing would be to introduce more detailed fluvial deposition modelling up to the point that actual channel belts and possibly, individual river channels are simulated. Sedsim has shown it is able to simulate channels displaying sinuosity and it might be possible to simulate individual fluvial channel and floodplain deposits. Such simulations would require increased temporal and spatial resolution to capture the features and might not be suitable for large basin-scale models. Yet, nested models with already increased spatial and temporal resolution might prove suitable.

6.1.3. Permeability model

A less bimodal porosity distribution, or more specifically, increased mid-range porosity value occurrence, would benefit the permeability model by increasing the mid-range permeability values, due to its direct link to porosity through the porosity-permeability transform. An additional improvement to the permeability model would be several facies-dependent porosity-permeability transforms for a single formation. This way, sandstone would return a different porosity-permeability relation than silts or clays. The entire formation based porosity-permeability transforms used in this study, includes all permeability data from a formation disregarding the type of facies, making it a rough average of the entire formation that is missing the more extreme values. The extreme values are likely to be most

important in defining seal and reservoir permeability or baffles to flow in migration assisted storage of CO_2. If a facies dependent transform is found, it could be implemented in reservoir modelling software by a simple conditional (if-then) statement based on the dominant grain size at that location in the Sedsim data.

6.1.4. Pseudo-gamma ray

The use of pseudo-wells with pseudo-gamma ray values allowed rapid comparisons between Sedsim generated model data and gamma-ray well data. This in turn, enabled an effective model-to-well tuning workflow. The combination of grain size and layer thickness dependency in the pseudo-gamma ray transforms resulted in better insight into and representation of the model, compared to using only one of the two dependencies in the transform. Yet, it is likely that much can be gained in refining the pseudo-gamma ray transforms. For example, it is unlikely that a 50/50 weighting to grain size and layer thickness is ideal, as it is more likely that one of the two should play a prominent role.

6.2. Potential GSC workflow applications

Geological sequestration of CO_2 (GSC) in deep aquifers is probably the most promising storage option for anthropogenic produced CO_2. In this type of storage, migration assisted storage (MAS) will likely be the dominant trapping mechanism because of the potential enormous storage capacity. To effectively calculate or estimate the possible geological storage capacities, comprehensive 3D models of the subsurface will be necessary over large areas. In this context, stratigraphic forward models like the Surat Basin model have four potential applications:

- Tool to identify and characterize potential GSC locations.
- Providing a geological framework for numerical flow modelling.
- Serving as a basis for more geologically realistic facies models used in conventional 3D geostatistic models of the subsurface.
- Part of a hybrid model, a stratigraphic forward model combined with a conventional 3D geostatistic model.

6.2.1. Identifying and characterizing potentially GSC locations

The ability of stratigraphic forward modelling to simulate likely distributions of (regional) seals and reservoirs could help identify and assess suitable locations for geological storage of CO_2. For example, in the EPQ-7 potential sequestration tenement, the Precipice Sandstone shows good porosity with 50% to 75% net to gross values, the overlying Evergreen Formation has thick low porosity, silt and mudstone intervals with net to gross values between 0% towards the northeast and 30% in the southwest. The sealing capability of the Evergreen Formation in the southwest of the nested model could be questioned due to the 30% sand content. The model shows that in this area, the sand bodies are interbedded with low porosity intervals and thus not likely to be connected vertically. In the model, this is caused by the formation of a large lake with constantly changing shorelines. During receding water levels sandy shorelines form which are flooded when water levels rise, followed by deposition of a fine grained interval.

After a potential GSC location is identified, the stratigraphic forward model can be used to predict likely sediment properties. Although the porosity and permeability distributions found in the model are too bimodal compared to observed values, the porosity values in the model-to-well logs show a very reasonable match, especially Pineview-1 in the EPQ-7 tenement (figure 5.6C). The model-predicted sediment properties for the EPQ-7 Nested Model meet the criteria set for GSC by Bradshaw et al. (2009):

- Considering the Lower and Upper Evergreen Formation an unconventional seal, the thickness would be well over 250 m over an area of 4800 km^2, compared to the 100 m over 2000 m^2 criteria.
- Sandstone intervals in the model generally have porosities of roughly 20% and permeability values between 40 and 170 mD, compared to the respective 10% and 10 mD criteria.

In conclusion,the results from the Surat Basin stratigraphic forward model suggest that the EPQ-7 tenement is a very suitable location for GSC, with the Precipice Sandstone acting as the reservoir and the Evergreen Formation forming the seal.

6.2.2. Geological framework for numerical flow modelling

The dynamic nature of migration assisted storage requires numerical flow models that help in estimating the CO_2 storage capacity and simulate migration of the injected CO_2 in prospective areas. A stratigraphic forward model can be used as a tool to rapidly produce a well data constrained static geological model, which can be directly imported into flow modelling software and serve as a framework for further numerical flow modelling. A good match with well data ensures that the model captures the important features of the subsurface for flow modelling. As a stratigraphic forward model can be constructed in a relative short time, the Surat Basin Stratigraphic Forward Model was constructed within six months by a novice modeller. Of these six months half was spend on studying literature of the basin and learning to use the Sedsim stratigraphic forward modelling package. An expert modeller will probably be able to build the same model with similar or better results in roughly three months.

6.2.3. Basis for geologically realistic facies models used in conventional 3D geostatistic models

At present, static 3D geological models of the subsurface are generally built in reservoir modelling software programs like Petrel from Schlumberger or RMS from Roxar. These programs make heavy use of geostatistics and upscaling techniques to predict properties away from wells. Geostatistical models use variograms as a basis for the simulation of the facies model and reservoir properties. In variograms the correlation of data decreases with distance between data points (wells). At a distance of zero from the data points the correlation is perfect, with increasing distance the correlation between points becomes equal to the overall variance of the total data.

Given that a modelled location has high well counts and density, geostatistical models can be very useful and return credible results, although even in locations with good well coverage geostatistical property and facies distributions often look slightly random and do not make geological sense. This is simply caused by the fact that the facies model and subsequent simulated properties are made to match statistical relations, not geological depositional processes. A stratigraphic forward model could help

make geostatistical models more realistic by using the stratigraphic forward model grain size or facies distributions as a framework in which the facies model is simulated. This could be done by importing the stratigraphic forward model results to the reservoir modelling software and make the geostatistical facies model take into account what type of grain size/facies is present at the exact same location in the stratigraphic forward model. Then, a function could be introduced that would increase the probability of the corresponding geostatistical facies occurring at that location.

6.2.4. Stratigraphic forward model/conventional 3D geostatistic model hybrid

In locations with limited well data a geostatistical model will only yield good results in the parts of the model which are in close proximity to the wells, in the rest of model the results will not be much better than the overall variance in the data. In these instances a stratigraphic forward model could potentially return better overall results. As variogram-based geostatistical models will always display a perfect match at the well locations, a stratigraphic forward model could only return better results at locations away from wells. In this situation, a hybrid of a geostatistical and stratigraphic forward model could return the best results: In areas close to wells, the geostatistical model is used and in data-poor areas away from wells, the stratigraphic forward model is used. This hybrid approach has recently been used in a GSC workflow for the Gippsland Basin in southeastern Australia by Miranda et al. (2012).

6.1.5. Surat Basin Zerogen Model

For the Zerogen CCS project, a geostatistic 3D model of the EPQ-7 tenement was made. Within the facies model the porosity and permeability models were simulated. Figure 6.1 shows a screenshot of the porosity model. Although it probably fits statistically to the well data, the distribution looks random and not much like the stratigraphic forward model results at the same location. This is probably enhanced by the fact that the area has poor well coverage with most of the wells dating from the 1960's to 1980's often without digital well logs. The Zerogen Static Model could potentially be improved by either, incorporating the Surat Basin Stratigraphic Forward Model in its facies model or by combining both models to create a hybrid model.

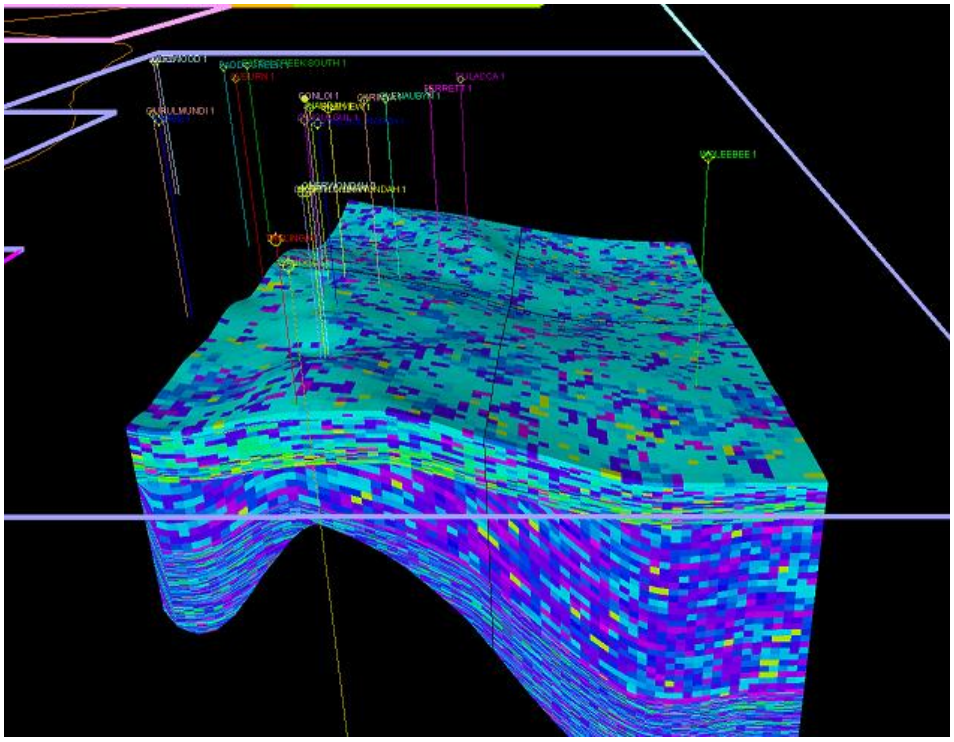

Figure 6.1: Surat Basin Zerogen Static Model of the EPQ-7 sequestration tenement (Zerogen Model provided by the Geological Survey of Queensland).

7. Conclusion

In order to assess and demonstrate the use of stratigraphic forward modelling (SFM) in rapidly generating a well-constrained static model and its potential use in generic GSC workflows, a SFM was built for the Precipice Sandstone, Evergreen Formation and Hutton Sandstone of the Surat Basin. This model, the Surat Basin Stratigraphic Forward Model, simulates the deposition and burial during the Early to Middle Jurassic over a period of 36 million years. In order to build the model efficiently, a workflow was used in which the model results could be directly compared to well data, allowing for an effective time efficient tuning process. This resulted in a good match with well data in the basin centre and EPQ-7 potential CO_2 sequestration tenement.

The porosity values generated with the model lie in the ranges found in well log derived porosity and seem to follow porosity trends in these wells. The model seems to roughly match in the pure sand and mud interval porosity, although a bimodal porosity distribution limits the model in correctly predicting the more intermediate porosity values. The model permeability values were generated from the model porosity values using a porosity-permeability transform. Although the model permeability values lie within the value range found in the basin, the model does not match the upper permeability values found in the Precipice Sandstone. From this it can be concluded that the porosity and permeability results from the model are very reasonable for a demonstration project, yet could use further refinement to reduce the bimodal distribution in the porosity and introduce facies specific porosity-permeability transforms to achieve more realistic permeability ranges.

The Surat Basin SFM could be used in a variety of potential applications in the GSC workflow:

- The model can help identify and characterize suitable locations for geological sequestration of CO_2 (GSC), as is demonstrated for the EPQ-7 CO_2 sequestration tenement.
- The model can be directly imported into reservoir modelling software and serve as a geological framework for numerical flow models.
- The model can be used in conjunction with conventional 3D geostatistical reservoir models; either by providing data in areas with poor well and/or seismic coverage, resulting in a SFM/geostatistic model hybrid, or by enhancing the facies model used in geostatistical models.

It should be noted that the Surat Basin SFM model:

- is mainly based on literature descriptions of the simulated formations, with limited use of well data;
- is built by a novice modeller in limited time;
- has a good match with the well data and reasonable porosity and permeability results;
- can be used in a variety of potential applications in further GSC workflows;

The primary conclusion is that this study demonstrates the high potential value of SFM, using Sedsim, in rapidly generating static reservoir models for use in GSC workflows, especially in areas with limited well data.

8. Acknowledgements

First of all, I would like to thank Cedric Griffiths and Karsten Michael for their valuable supervision, guidance and assistance and for giving me the opportunity to come to Perth and work on this project. I would like to thank Chris Spiers for contacting CSIRO and for his supervision in Utrecht. The Australian Government is thanked for providing the funding through its CRC Program to support this CO2CRC research project. Furthermore, I thank Mike McKillop and Jonathan Hodgkinson from the Geological Survey of Queensland, for the data they provided and the wonderful fieldtrip to the Surat Basin. Finally, I thank everybody at CSIRO that helped me out and made my stay enjoyable, especially: Christine Trefry, Chris Dyt, Sunil Varma and my fellow students.

9. References

Allen, R.J., 1976: *Surat Basin*. In: Leslie, R.B., Evans, H.J. & Knight, C.L., (editors): Economic Geology of Australia and Papua New Guinea, 3, Petroleum. Australasian Institute of Mining and Metallurgy, Monograph Series 7,pp. 266–272.

Bachu, S., Bonijoly, D., Bradshaw, J., Burruss, R., Holloway, S., Christensen, N.P.,Mathiassen, O.M., 2007: *CO_2 storage capacity estimation: methodology and gaps*., Int. J. Greenhouse Gas Control 1, pp. 430–443.

Battersby, D.G. 1981. *New discoveries in the Bowen/Surat Basin*. APEA Journal 21, 2, 39-44.

Bradshaw, B.E., Spencer, L.K., Lahtinen, A.C., Khider, K., Ryan, D.J., Colwell, J.B., Chirinos, A.,Bradshaw, J. 2009: *Queensland carbon dioxide geological storage atlas.* Compiled by Greenhouse Gas Storage Solutions on behalf of Queensland Department of Employment, Economic Development and Innovation.

Brakel, A.T. 1992: *Sequence boundaries and sequences in the Taroom region*. In: Totterdell J.M., Wells, A.T., Brakel A.T., Korsch R.J. & Nicoll M.G, (editors): Sequence stratigraphic interpretation of seismic data in the Taroom region, Bowen and Surat Basins, Queensland*.,* Bureau of Mineral Resources Record 1991/102, pp. 11–22.

Browne, G.H. & Hart, B.S., 1990: *Discussion: Hummocky cross-stratification from the Boxvale Sandstone Member in the northern Surat Basin, Queensland.*, Australian Journal of Earth Sciences, 37, pp. 377–378.

Butcher, R. 1992: *A-P 257P - 499P Western Surat Basin, Evergreen sands study.*, Company exploration report. Queensland Digital Exploration Reports (QDEX). Geological Survey of Queensland.

Cadman, S.J., Pain, L. & Vuckovic, V. 1998: *Bowen and Surat Basins, Clarence-Moreton Basin, Gunnedah Basin, and other minor onshore basins.*, Queensland, NSW and NT, Australian Petroleum Accumulations Report 11, Bureau of Resource Sciences, Canberra.

de Caritat, P., Braun, J., 1992: *Cyclic development of sedimentary basins at convergent plate margins — 1. Structural and tectono-thermal evolution of some gondwana basins of eastern Australia.* Journal of Geodynamics, 16, 4, pp. 241-282

Elliott L.G. & Brown R.S. 1988: *The Surat and Bowen Basins – a historical review*., In: Australian Petroleum Exploration Association (editor): petroleum in Australia: the first century., pp.120-138.

Elliott L.G. 1989. *The Surat and Bowen Basins.,* APEA Journal 29, 1, pp. 398-416.

Elliott L.G. 1993*. Post-Carboniferous tectonic evolution of eastern Australia.,* APEA Journal 33, pp. 215–236.

Exon, N.F., 1976: *Geology of the Surat Basin in Queensland*., Bureau of Mineral Resources Bulletin, 1, 166

Fielding, C.R., 1989: *Hummocky Cross-Stratification from the Boxvale Sandstone Member in the Northern Surat Basin, Queensland.* Aust.J.Earth Sci., 36, 3, pp. 469-471

Fielding, C.R., Gray, A.R.G., Harris, G.I. Salomon, J.A., 1990: *The Bowen Basin and overlying Surat Basin*., In: D.M. Finlayson (Compiler and editor), The Eromanga-Brisbane Geoscience Transect: A guide to basin development across Phanerozoic Australia in southern Queensland. Bureau of Mineral Resources, Geology & Geophysics, Bulletin 232, pp. 105–116.

Frogtech, 2005: *OZ SEEBASE study 2005*, public domain report to Shell Development Australia by Frog Tech Pty Ltd.

Gallagher, K., 1990: *Permian to Cretaceous subsidence history along the Eromanga–Brisbane Geoscience Transect.*, 133-151, Bureau of Mineral Resources, Bureau of Mineral Resources Bulletin 232.

Gallagher, K.; Dumitru, T. A. , Gleadow, A. J. W., 1994: *Constraints on the vertical motion of eastern Australia during the Mesozoic*. Basin Research, 6, 2-3, pp. 77-94.

Griffiths, C.M., Paraschivoiu, E., 1998: *Three-dimensional forward stratigraphic modelling of early Cretaceous sedimentation on the Leveque and Yampi shelves, Browse Basin.* APPEA Journal 38, 1, 147-158.

Griffiths, C.M., 2001: *Stratigraphic forward modelling short course: Brief review of stratigraphic forward modelling*. CSIRO Petroleum.

Griffiths, C.M., Dyt, C., 2001: *Six years of Sedsim exploration applications* (abs.). AAPG Bulletin 85, 13.

Griffiths, C.M., Dyt, C., Paraschivoiu, E., Liu, K. 2001: *Sedsim in hydrocarbon exploration*. In: Merriam, D., Davies, J.C. (editors), Geologic Modelling and Simulation. Kluwer Academic, pp. 71-97.

Griffiths, C.M., 2008: S*tratigraphic forward modelling and Sedsim,* CSIRO petroleum.

Gluyas, J., Cade, C.A., 1997: *Prediction of porosity in compacted sands*., In: Kupercz, J.A., Gluyas, J., Bloch, S. (editors), Reservoir qualiy prediction in sandstones and carbonates, AAPG Memoir 69, pp. 19-28.

Golin,V., Smyth, M., 1986: *Depositional environment and hydrocarbon potential of the Evergreen Formation; ATP 145P, Surat Basin,Queensland.* APEA journal, 26, 1, pp. 171

Gray, A.R.G., 1972: *Stratigraphic drilling in the Surat and Bowen Basins 1967–70*. Geological Survey of Queensland, Report, 71.

Green, P.M., Carmicheal, D.C., Brain, T.J., Murray, C.G., McKellar, J.L, Beeston, J.W., Gray, A.R.G., 1997: *Lithostratigraphic units in the Bowen and Surat Basins, Queensland.,* In: Green, P.M. (editor): The Surat and Bowen Basins, Minerals and Energy Review Series, Queensland Department of Mines and Energy, pp. 41-108.

Hodgkinson, J., Grigorescu, M., 2012: Background research for selection of potential geostorage targets—casestudies from the Surat Basin, Queensland, Australian Journal of Earth Sciences: An International Geoscience Journal of the Geological Society of Australia, 60, 1, pp. 71-89.

Hoffman, K.L., Green, P.M.; Gray, A.R.G. *Stratigraphic implications of seismic-based sequence stratigraphy.,* In: Green, P.M. (editor): The Surat and Bowen Basins, Minerals and Energy Review Series, Queensland Department of Mines and Energy, pp. 41-136.

Hoffmann, K.L., Totterdell, J.M, Dixon, O., Simpson, G.A., Brakel, A.T., Wells, A.T., Mckellar, J.L., 2009: *Sequence stratigraphy of Jurassic strata in the lower Surat Basin succession, Queensland.* Aust.J.Earth Sci., 56, 3, pp. 461-476.

Huang, X., Dyt, C., Griffiths, C.M., Salles, T., 2012:*Numerical forward modelling of 'fluxoturbidite' flume experiments using Sedsim.,* Marine and Petroleum Geology, 35, pp. 190-200.

Korsch, R.J., Totterdell, J.M., 2009: *Subsidence history and basin phases of the Bowen, Gunnedah and Surat Basins, eastern Australia.* Aust.J.Earth Sci., 56, 3, pp. 335-353.

Li, F., Dyt, C., Griffiths, C., and McInnes, K., 2007: *Predicting seabed change as a function of climate change over the next 50 years in the Australian southeast.* In: Harff, J., Hay, W.W, Tetzlaff, D.M.(editors), Coastline Changes: Interrelation of Climate and Geological Processes, Geological Society of America, pp. 43–64.

Li, F., Griffiths, C.M., Dyt C.P., Weill, P., Feng, M., Salles,T. Jenkins, C., 2009: *Multigrain seabed sediment transport modeling for the south-west Australian Shelf.* Marine and Freshwater Research, 60, pp. 774-785.

Michael, K., Arnot, M., Cook, P., Ennis-King, J., Funnell, R., Kaldi, J.G., Kirste, D., Paterson, L., 2009: *CO2 storage in saline aquifers I—current state of scientific knowledge.* Energy Procedia 1, pp. 3197–3204.

Marshallsea S. 1985: *Thermal history of the Bowen Basin, Queensland: an apatite fission track study.,* PhD thesis, University of Melbourne,(unpubl.)

Martin, K.R. 1981: *Deposition of the Precipice Sandstone and the evolution of the Surat Basin in the early Jurassic.* APEA journal, 21, 1, pp. 16-23.

Miranda, J., Eid, R., McLean, M. O'Brien, G., Griffiths, C.M., Dyt, C., Salles, T., Tingate, P., Goldie Divko, L. Campi, M., 2012: *Gippsland Basin stratigraphic and CO2 migration modelling: workflows for building regional, geological carbon storage (GCS) reservoir models*. Proceedings of the Fourth Eastern Australasian Basins Symposium and Exhibition (EABS IV), Brisbane, Australia, 11-14 September 2012.

Mitrovica, J.X., Beaumont ,C., Jarvis ,G.T. 1989: *Tilting of continental interiors by the dynamical effects of subduction.* Tectonics, 8, 5, pp. 1079-1094.

Mollan, R.G., Forbes, V.R., Jensen, A.R., Exon, N.F. & Gregory, C.M., 1972: *Geology of the Eddystone, Taroom and western part of the Mundubbera Sheet areas, Queensland.,* Bureau of Mineral Resources, Geology and Geophysics, Australia, Report 142

Paraschivoiu E., Griffiths C. M., Dyt C., Carter S., 2000: *The use of three-dimensional nested forward stratigraphic simulations to provide variable-scale heterogeneity models*. Proceedings of the Upscaling Downunder Symposium, Melbourne.

Power, P.E., Devine, S.B., 1970: *Surat Basin, Australia - Subsurface Stratigraphy, History, and Petroleum.* Am.Assoc.Pet.Geol.Bull., 54, 12, pp. 2410-2437.

Phillips, B.J. and Carne G.E., 1982: *Goodar Seismic Survey ATP's 243P/250P Surat Basin, Queensland.,* Company exploration report. Queensland Digital Exploration Reports (QDEX). Geological Survey of Queensland.

QCGI 2009. *Potential for carbon geostorage in the Taroom Trough, Roma Shelf and the Surat, Eromanga and Galilee Basins – Preliminary Report.*, Geological Survey of Queensland Carbon Geostorage Initiative.

Raza, A., Hill, K.C., Korsch, R.J., 2009: *Mid-Cretaceous uplift and denudation of the Bowen and Surat Basins, eastern Australia: relationship to Tasman Sea rifting from apatite fission-track and vitrinite-reflectance data.*, Australian Journal of Earth Sciences, 56, pp. 501–531.

Salles, T., Marchès, E., Dyt, C., Griffiths, C.M., Hanquiez, V., Mulder, T., 2010: *Simulation of the interactions between gravity processes and contour currents on the Algarve Margin, South Portugal. using the stratigraphic forward model Sedsim*. Sediment. Geol. 229, pp. 95-109.

Sell, B.H., Brown, L.N. & Groves, R.D, 1972: *Basal Jurassic sands of the Roma area*. Queensland Government Mining Journal, 71, pp. 301-303.

Sclater, J.G., Christie, P.A.F., 1980: *Continental Stretching: An explanation of the Post-Mid-Cretaceous subsidence of the Central North Sea Basin*., Journal of geophysical research, vol. 85, no. B7, pp. 3711-3739.

Tabassi. A., 1986: *ATP 328P & Environments Goondiwindi Fault zone study.,* Company exploration report. Queensland Digital Exploration Reports (QDEX). Geological Survey of Queensland.

Terzaghi, K., 1936: *The shear resistance of saturated soils*., Proceedings for the 1st international conference on Soil Mechanics and Foundation Engineering, Cambridge MA, 1, pp. 54 -56.

Terzaghi, K., Peck, R.B., 1948: *Soil Mechanics in Engineering Practice*, pp. 566.

Tetzlaff, D. Harbaugh, J. 1989: *Simulating Clastic Sedimentation:Computer Methods in the Geosciences*., VanNostrand Reinhold, New York, 202 pp.

Waschbusch, P, Korsch, R.J., Beaumont, C., 2009: *Geodynamic modelling of aspects of the Bowen, Gunnedah, Surat and Eromanga basins from the perspective of convergent margin processes.* Aust.J.Earth Sci., 56, 3, pp. 309-334.

Wijns, C., Poulet, T., Boschetti, F., Dyt C., Griffiths, C.M., 2004: *Interactive Inverse Methodology Applied to Stratigraphic Forward Modelling*., Geological Society, Special Publications January 1, 2004, v. 239, pp. 147-156.

Wiltshire, M.J., 1989: *Mesozoic stratigraphy and palaeogeography, eastern Australia*., In: O'Neil B.J.(editor): The Cooper and Eromanga Basins, Australia., Proceedings of Petroleum Exploration Society of Australia, Society of Petroleum Engineers, Australian society of Exploration Geophysics (SA Branch), Adelaide, pp. 279-291.

Totterdell, J.M.; Moloney, J.; Korsch, R.J.; Krassay, A.A., 2009: *Sequence stratigraphy of the Bowen-Gunnedah and Surat Basins in New South Wales*. Aust.J.Earth Sci., 56, 3, pp. 433-459.